LEVEL I

1.2

UNDERWATER ACOUSTIC ABSORPTION CHARACTERISTICS OF COMPOSITES OF WOOD, RUBBER, AND STEEL

F. A. Barge

Technical Memorandum
File No. TM 78-52
May 1978
Contract No. N00017-73-C-1418

Copy No. 55

The Pennsylvania State University
APPLIED RESEARCH LABORATORY
Post Office Box 30
State College, PA 16801

NAVY DEPARTMENT

NAVAL SEA SYSTEMS COMMAND

UNCLASSIFIED

SECURITY CLASSIFICATION OF THIS PAGE *(When Data Entered)*

(14) ARL/PSU

REPORT DOCUMENTATION PAGE

READ INSTRUCTIONS BEFORE COMPLETING FORM

1. REPORT NUMBER: TM-78-52	2. GOVT ACCESSION NO.
3. RECIPIENT'S CATALOG NUMBER	
4. TITLE (and Subtitle): (6) UNDERWATER ACOUSTIC ABSORPTION CHARACTERISTICS OF COMPOSITES OF WOOD, RUBBER, AND STEEL	5. TYPE OF REPORT & PERIOD COVERED: (9) Technical Memorandum
	6. PERFORMING ORG. REPORT NUMBER
7. AUTHOR(s): (10) F. A. Barge	8. CONTRACT OR GRANT NUMBER(s): (15) N00017-73-C-1418
9. PERFORMING ORGANIZATION NAME AND ADDRESS: Applied Research Laboratory, Post Office Box 30, State College, PA 16801	10. PROGRAM ELEMENT, PROJECT, TASK AREA & WORK UNIT NUMBERS
11. CONTROLLING OFFICE NAME AND ADDRESS: Naval Sea Systems Command, Washington, DC 20362, Code 035	12. REPORT DATE: (11) May 1978
	13. NUMBER OF PAGES: 72
14. MONITORING AGENCY NAME & ADDRESS *(if different from Controlling Office)*: (12) 76 p.	15. SECURITY CLASS. *(of this report)*: UNCLASSIFIED
	15a. DECLASSIFICATION/DOWNGRADING SCHEDULE

16. DISTRIBUTION STATEMENT *(of this Report)*

Approved for public release. Distribution unlimited.
As Per NAVSEA - April 4, 1978.

17. DISTRIBUTION STATEMENT *(of the abstract entered in Block 20, if different from Report)*

18. SUPPLEMENTARY NOTES

19. KEY WORDS *(Continue on reverse side if necessary and identify by block number)*

underwater
acoustic
absorption
wood
rubber
steel

20. ABSTRACT *(Continue on reverse side if necessary and identify by block number)*

In this experimental investigation, the underwater acoustic absorption characteristics of composites of various species of wood, rubber, and steel were determined under low hydrostatic pressure and over a frequency range of 10 to 50 kHz. The test samples included a thin steel plate, closed-cell bubble rubber (Rubatex), hemlock, fir plywood, white pine, redwood and Saper-T rubber. Composites of these materials were tested in a semi-anechoic water tank, where the technique used to determine the incident and reflected

(CONT.

DD FORM 1 JAN 73 1473 EDITION OF 1 NOV 65 IS OBSOLETE

UNCLASSIFIED

SECURITY CLASSIFICATION OF THIS PAGE *(When Data Entered)*

391 007

(B)

CONT'

20. pressure amplitudes was the tone-burst method. The complex reflection factor for normal incidence, calculated from the standing waves measured in front of each sample at discrete frequencies, was determined for each composite over the frequency range of interest. The bubble rubber-steel composite was found to have the highest reflection factor over the frequency range of measurement; however, when reversed (steel-bubble rubber), very low reflection factors were measured, but the data were difficult to repeat. Consistently low reflection factors ($R \approx 0.5$) were measured for the fir plywood-steel-bubble rubber composite and for the Saper-T rubber-steel-bubble rubber composite. In general, the other soft woods evaluated were found to be resonant-type absorbers, although the broadband reflection factor did decrease by approximately 20 to 30 percent when a layer of Saper-T rubber was included in the composite.

approx.

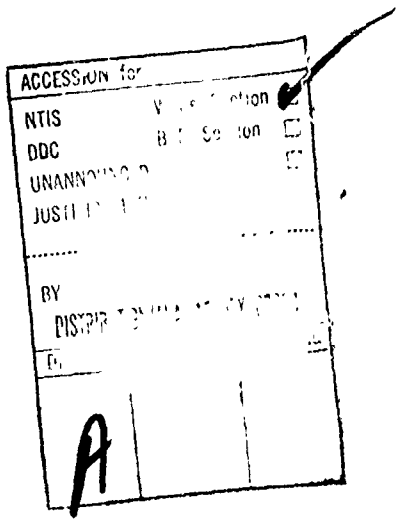

ABSTRACT

In this experimental investigation, the underwater acoustic absorption characteristics of composites of various species of wood, rubber, and steel were determined under low hydrostatic pressure and over a frequency range of 10 to 50 kHz. The test samples included a thin steel plate, closed-cell bubble rubber (Rubatex), hemlock, fir plywood, white pine, redwood and Saper-T rubber. Composites of these materials were tested in a semi-anechoic water tank, where the technique used to determine the incident and reflected pressure amplitudes was the tone-burst method. The complex reflection factor for normal incidence, calculated from the standing waves measured in front of each sample at discrete frequencies, was determined for each composite over the frequency range of interest. The bubble rubber-steel composite was found to have the highest reflection factor over the frequency range of measurement; however, when reversed (steel-bubble rubber), very low reflection factors were measured, but the data were difficult to repeat. Consistently low reflection factors ($R \simeq 0.5$) were measured for the fir plywood-steel-bubble rubber composite and for the Saper-T rubber-steel-bubble rubber composite. In general, the other soft woods evaluated were found to be resonant-type absorbers, although the broadband reflection factor did decrease by approximately 20 to 30 percent when a layer of Saper-T rubber was included in the composite.

TABLE OF CONTENTS

LIST OF ILLUSTRATIONS

LIST OF TABLES

LIST OF SYMBOLS

$\bar{A}$	incident pressure amplitude
$\bar{B}$	reflected pressure amplitude
$\bar{P}$	amplitude of acoustic pressure
P_{max}	maximum amplitude of acoustic pressure
P_{min}	minimum amplitude of acoustic pressure
$\bar{R} = \bar{B}/\bar{A}$	Reflection factor
X_{min}	distance of the first or second pressure minimum from the sample surface
$\bar{Z}$	complex impedance
c	sound velocity in sample material
c_0	sound velocity in water
f	frequency
$i = \sqrt{-1}$	imaginary unit number
$k = \omega/c$	wavenumber in a sample material
$\lambda = c_0/f$	wavelength
ξ	normalized impedance
ρ_0	density of fluid medium
ρ	measured density of sample material
σ	phase shift
ϕ	phase angle
$\omega = 2\pi f$	angular frequency

ACKNOWLEDGMENTS

The author wishes to extend thanks to the Chairman of the Acoustics Program, Dr. Jiri Tichy, for his support and encouragement, to advisor Dr. Gerald Lauchle for his guidance and assistance in the development of this research, to assistant Jeffrey Oakly who helped with the experimental procedures and contributed to this presentation, and to the many staff members at The Garfield Thomas Water Tunnel of the Applied Research Laboratory at The Pennsylvania State University, whose assistance has contributed a great deal to the completion of this study.

Further appreciation is expressed to the staff at the Forestry Research Laboratory, especially Dr. Paul R. Blankenhorn and Dr. Wayne K. Murphey, for their time and assistance in the use of their facilities.

This effort has been supported by the Applied Research Laboratory at The Pennsylvania State University under contract with the Department of the Navy, Naval Sea Systems Command, Code 035.

CHAPTER I

INTRODUCTION

1.1 Origin and Importance of the Investigation

In order to improve the hydroacoustic measurement capability in the Garfield Thomas 48-inch diameter Water Tunnel located at the Applied Research Laboratory of The Pennsylvania State University, efforts to reduce background noise and in-tunnel reverberation must be considered. This report will treat the latter problem in detail. Removable tunnel test section liners have been designed and used for hydrodynamic purposes for many years. It is feasible, therefore, to design and install a liner specifically for the reduction of acoustic reflection. Before such a liner can be fabricated, however, the material with which it is to be made must be determined. This investigation is designed to determine experimentally which material or combination of materials minimizes acoustic reflection of underwater sound in the frequency range where the dominant type of reverberation in the tunnel is due to standing radial waves. For many of the hydroacoustic investigations performed in the Garfield Thomas Water Tunnel the frequency range most commonly used is 5-50 kHz. However, the water tank which was available for the present experiments had linear dimensions which were too small relative to the wavelengths produced at frequencies below 10 kHz for practical measurements to be made. Consequently, the frequency range considered is 10-50 kHz for normal incidence only.

The most pertinent literature on the sound absorption characteristics of woods, rubbers, metals, and combinations thereof, are listed in the Bibliography. Although sound absorption characteristics of wood were previously investigated by Lastinger [12], the measurements were made in the frequency range 3-8 kHz and at hydrostatic pressures to 10,000 psi. The measured change in acoustic characteristics with hydrostatic pressure was found to be negligible. The present investigation covers the frequency range 10-50 kHz at near-atmospheric pressures in which data have not appeared in the open literature.

In Germany, a group working under Meyer [15] investigated the absorption of underwater sound for rubber broadband absorbers used as tank liners. They developed a plastic wedge made of Fafnir [15] which consisted of three rubber layers cemented together with the middle layer containing punched cylindrical (air-filled) holes. Reflections are reduced by a mechanism of sound dissipation. An early form of Fafnir was made from a synthetic rubber containing materials, such as sawdust or cork-dust, with high air content. In time, it tended to absorb water which caused its absorption properties to degrade. Similarly, a material made from a damp mixture of pine dust and Portland cement, Insulkrete [7], was developed by the United States Navy to resemble viscous-type absorbers. In this case, acoustic dissipation occurs because of the relative motion between the water which penetrates the surface and the material. The B. F. Goodrich Company developed SOAB [9], a metal-loaded rubber (a mixture of rubber and metallic powder), which increased attenuation more than rubber alone and offered a better acoustic impedance match with water than

porous rubber or mixtures of rubber with either sawdust or cork. Metal-loaded butyl rubber has the best overall abosorption characteristics as compared with plain rubber, Fafnir, Insulkrete, and canvas.

In addition to these broadband absorbers, thin "tuned" rubber absorbers were developed for use as coatings and liners and were bonded to a rigid backing. This type of composite may be considered as a lumped-element complex impedance, with resistive and reactive (mass) components. B. F. Goodrich [9] also developed Saper T, a modified version of the "tuned" rubber (Alberich) developed by Meyer and associates [15].

The importance of the present underwater measurements is to provide data for the design of a liner to reduce reverberation in the test section of the 48-inch diameter Water Tunnel. In order to augment the absorption data noted previously, the underwater absorption characteristics of bubble rubber (a nitrogen-filled, closed-cell rubber), soft woods such as hemlock, fir plywood, white pine, and redwood, a modified version of Saper rubber and combinations of these materials are evaluated as possible anechoic treatments.

1.2 Statement of Problem

The purpose of this investigation is to experimentally determine the underwater acoustic absorption characteristics of composites of various species of wood, rubber, and steel under near-atmospheric hydrostatic pressure.

1.3 Method of Investigation

There are a number of methods available for determining underwater acoustic absorption characteristics. The tone-burst technique [4] is most suitable for our frequency range because it allows determination of the free-field incident and reflected pressure amplitudes while still within the confines of a laboratory test tank. If one were to perform similar measurements at lower frequencies, an impedance tube apparatus would be recommended. The tube technique is not applicable here because the diameter would have to be on the order of one-tenth of an inch to assure plane wave propagation at the higher frequencies.

The complex absorption coefficient for normal incidence is determined on the basis of standing waves measured in front of the test sample. In a water tank, a sinusoidal pulse travels from a sound source (projector) towards the test material at an angle normal to its surface. The pulse is partially reflected and partially transmitted at the surface of the test material. The field in front of the sample is determined by scanning with a receiving hydrophone. At a given frequency, the spatial sound field in front of the reflector is in the form of a sinusoid, i.e., a standing wave field is set up. The reflected wave and the fraction, R, of the incident wave combine to build up this standing wave pattern where R is the complex reflection factor. Therefore, by measuring the standing wave pattern in front of the reflector, one can obtain the reflection factor. A traversing hydrophone (receiver) is used to measure the pulse amplitude and phase after reflection from the fixed sample as a function of distance from the plane of reflection.

In order to reduce the interference effects due to reflection from the tank walls and free-surface, a B & K gating system Type 4440 is used. This gating system electronically eliminates the echoes caused by the boundaries of the enclosure so that free-field conditions are artificially achieved. The projector is driven with short pulses of a single-frequency signal. The projector and receiving system are gated so that only the desired acoustic signal from the generated pulse is received for processing.

The various materials in which the absorption characteristics are to be determined are attached to a 1/4-inch-thick steel plate which fits inside the water tank (Figure 1) close to one of the walls. The projector is suspended from a bar that rests on top of the tank while the receiver is connected to a traversing mechanism, making it mobile.

Previous researchers (see, for example, Waterhouse [24]) have found that reliable absorption measurements can be made in a water tank, provided the acoustic wavelength does not become larger than one-quarter of the minimum linear dimension of the tank. With this criterion, the lowest frequency that can be considered for the tank used in this investigation is 5 kHz. However, the distance from the source to the test sample is also a critical length. This length was chosen so that no reflections other than those originating from the test sample would be sensed by the receiver at a given time. This distance turned out to be less than the minimum linear dimension of the tank, thus requiring the minimum frequency to be set at 10 kHz.

CHAPTER II

DESCRIPTION OF EQUIPMENT

2.1 The Water Tank

The water tank (Figure 1) is constructed of wood with appropriate dimensions for the frequency range of interest. The inner dimensions of the tank are approximately 8 feet long, 4 feet wide and 4 feet deep. To prevent leakage, its interior sides are coated with epoxy, a layer of fiberglass, and a layer of rubber squares. As a final precaution to reassure that there would be no flow of water out of the tank, it was necessary to insert a polyethylene swimming pool liner. After construction, the tank was filled with fresh water. The water was changed periodically, because the tank has no water circulation or filtering equipment. The angle-iron and wood rim surrounding the water tank is 6 inches wide and supports bars in which the test material, the reference plate, and the hydrophones are suspended.

2.2 Test Materials

a. Steel Plate. Various composites in which the acoustic characteristics are to be measured are attached to a 1/4-inch-thick steel plate, approximately 47 inches high by 46 inches wide. Cylindrical holes of 3/16-inch diameter are drilled through the steel for purposes of attaching the wood samples. The steel plate is suspended from a steel bar 66 inches long which is welded to its upper edge. It remains in a vertical position parallel to the 4 foot tank walls. A U-bolt is fastened to the middle of the bar which enables a crane to lift the steel plate in and out of the water tank.

b. Bubble Rubber [9]. A sheet 3/8-inch thick, 45-3/8 inches wide and 42 inches high is attached to the steel plate with an industrial adhesive called Pliobond (a Goodyear product). This rubber is a nitrogen-filled, closed-cell rubber (trade name, Rubatex). It is soft, flexible, and light in weight, where its maximum absorption of water by volume is one percent.

c. Soft Woods [18]. (1) White Pine, Hemlock and Redwood: These plane samples are 3/4-inch thick commercially available stock, 45 inches high, and of random widths. They are arranged vertically (Figure 2b) on the reference plate allowing a 1/8-inch to 1/4-inch gap between each plank for swelling. The distinctive properties common to these woods are their straightness of grain and their uniformity of texture. Hemlock is the heaviest, while redwood is the lightest. All the panels are attached to the plate from the back side (relative to the incident pulse) with several uniformly spaced, 3/4-inch, #8 flat head brass wood screws. (2) AB Exterior Grade Fir Plywood: This sheet of plywood, 3/4-inch thick, 45 inches wide and 45 inches high is also attached to the steel plate in the same manner as the wooden panels. This plywood is fine-grained, uniformly textured, moderately soft and smoothly sanded.

d. Saper-T Rubber. A sheet of this commercially produced material 1/4-inch thick, 30 inches wide and 30 inches high is bonded to the steel plate with contact cement. Saper-T has been developed especially for anechoic tank lining applications. The manufacturer [9] claims that it provides 10 dB echo reduction for frequencies as low as 500 Hz. Its geometric configuration is shown in Figure 3.

2.3 Composites

a. Two-Layered Media. Because all the test samples are attached to the reference plate with either the bubble rubber or the steel plate as a backing, the acoustic absorption characteristics of this two-layered composite will be determined (Figure 2a).

b. Three-Layered Media. The three-layered media consists of a species of wood or Saper-T rubber attached to either the steel or bubble rubber side of the reference plate (Figure 2b). The wooden samples were attached to the reference plate making sure that the receiver would not be traversed near cracks between two adjacent planks, near knots, or near any other irregularity on the surface. If these precautions were not followed, the incident signal was diffracted and caused erroneous readings.

c. Four-Layered Media. Before attaching the wooden samples to the reference plate, a sheet of Saper-T rubber is bonded to the steel. The same experimental procedures are used for testing these composites, except that now the ordering of materials (Figure 2c) is wood, Saper-T rubber, steel, and bubble rubber.

2.4 Instrumentation

The test console is located in the Garfield Thomas Water Tunnel. In addition to the gating system, the console contains a power amplifier, two transducers, an oscilloscope, an oscillator, a traversing mechanism, a digital voltmeter, and a multimeter. A block diagram of the circuitry used in this investigation is shown in Figure 4.

Sine waves are generated by a Hewlett-Packard Wide Range Oscillator which drives the Model 4440 B & K Gating System. The gating

system converts the steady-state sinusoidal wave into pulses of predetermined width and repetition rate which serves as input to the projector after amplification by a Krohn-Hite power amplifier. The projector is thus operated in a pulsed mode over the frequency range of 10 to 50 kHz. A Celesco Corporation LC-10 hydrophone which is mounted on a traversing mechanism receives the direct and reflected signals. This mechanism allows the receiving hydrophone to move perpendicularly to the surface of the sample and is equipped with a turn indicator. One complete revolution amounts to a displacement of 1/20-inch for the receiver. It is turned manually to avoid extraneous background noise incurred by using a motor. The received signal is amplified and passed to both the oscilloscope and to the signal input of the receiving gating system. The time between pulses is adjusted such that all reflections in the tank subside before the next pulse is generated. The receiver gate is set to correspond to that period of time during which only the direct signal is present. In this way, tank wall and free surface reflections are eliminated from the experimental data. The average value of the gated voltage is held at a DC level for the duration of each pulse and displayed on a digital voltmeter, as well as on a multimeter. Because of its fast response time, the multimeter is used to detect the maximum and minimum voltages as the receiver is traversed. Once these voltages are located, the integrating voltmeter is used to find their precise values. The distance of the pressure minima are calculated directly from the turn indicator. These distances are then used to calculate the phase shift at the point of reflection.

CHAPTER III

THEORETICAL DATA REDUCTION

3.1 Reflection Factor and Phase Angle

The objective of this investigation, as stated in Section 1.2, is to determine experimentally the underwater acoustic absorption characteristics of composites of wood, rubber, and steel. The method requires probing the standing wave in front of the sample to determine both the magnitude and phase of the reflected pressure amplitudes. When plane waves transmitted in the water interfere with the waves reflected from the surface of the test sample, a standing wave pattern is generated in front of the test sample. From measurements of the spatial patterns of the pressure amplitude in the standing wave field (Figure 5), one can calculate the reflection factor and the phase angle.

Consider the case of partial reflection [22], where a reflecting surface absorbs some of the incident energy so that the reflected wave will be smaller in amplitude than the incident wave. The pressure at a point in Medium I (Figure 6) is given by:

$$\overline{P} = p_i + p_r = \overline{A}e^{i(\omega t + kx)} + \overline{B}e^{i(\omega t - kx)} \quad , \qquad (3.1)$$

where p_i = the incident pressure, p_r = the reflected pressure and where $\overline{A}$ and $\overline{B}$ are the complex pressure amplitudes of the incident and reflected waves, respectively; k is the wavenumber, and ω is the circular frequency. Let Equation (3.1) be represented by:

$$\overline{P} = \overline{A}(e^{ikx} + \overline{R}e^{-ikx})e^{i\omega t} \quad . \qquad (3.2)$$

The ratio $\overline{R} = \overline{B}/\overline{A}$ defines the reflection factor at the water/sample interface. Expanding the exponential functions of Equation (3.2) in terms of sines and cosines, then adding and subtracting $\overline{R}$ cos kx, one obtains the following equation:

$$\overline{P} = \overline{A}[2\overline{R} \cos kx + (1 - \overline{R})e^{ikx}] \quad , \tag{3.3}$$

where $2\overline{AR}$ cos kx represents a standing wave, and the time dependence has been suppressed. Let

$$\overline{R} = |\overline{R}|e^{-i\pi\sigma} = Re^{-i\pi\sigma} \quad , \tag{3.4}$$

where $-\pi\sigma$ represents the phase, then $\overline{P}$ can be written as the remaining fraction of the incident wave:

$$\overline{P} = \overline{A}[e^{ikx} + \overline{R}e^{-i(\pi\sigma + kx)}] \quad . \tag{3.5}$$

The magnitude of $\overline{P}$ is:

$$|\overline{P}| = |\overline{A}| \sqrt{1 + R^2 + 2R \cos 2(kx + \pi\sigma/2)} \quad . \tag{3.6}$$

By substituting $\pi\sigma/2 = k\sigma x/4 = 2\pi f\sigma\lambda/4c_0$, where λ is the wavelength, c_0 is the sound speed in water and f is the frequency, Equation (3.6) becomes:

$$|\overline{P}| = |\overline{A}| \sqrt{1 + R^2 + 2R \cos 2k(x + \sigma\lambda/4)} \quad . \tag{3.7}$$

The maximum of $|\overline{P}|$ occurs when cos $2k(x + \sigma\lambda/4) = -1$. Thus, the ratio of the maximum to minimum pressure amplitude is

$$d = \frac{\sqrt{1 + R^2 + 2R}}{\sqrt{1 + R^2 - 2R}} = \frac{1 + R}{1 - R} \quad . \tag{3.10}$$

and the magnitude of the reflection factor is:

$$R = \frac{d - 1}{d + 1} \quad . \tag{3.11}$$

The phase change during reflection determines the position of the minimum. The first minimum is given by:

$$2k(x_{min} + \sigma\lambda/4) = \pi \quad . \qquad (3.12)$$

Rearranging this equation in terms of σ we find that

$$\sigma = \left(\frac{\pi}{2k} - \frac{4x_{min}}{\lambda}\right)\frac{4}{\lambda} \quad . \qquad (3.13)$$

By substituting $k = 2\pi/\lambda$ into Equation (3.13) we get

$$\sigma = (1 - 4x_{min}/\lambda) \quad . \qquad (3.14)$$

The phase shift $-\pi\sigma$ can be represented by:

$$\phi = (4x_{min}/\lambda - 1)\pi \quad . \qquad (3.15)$$

The following rules [22] were applied to characterize the surface in terms of the phase angle, ϕ, and the reflection factor, R. For a completely absorbent surface, R equals zero; for a strongly absorbent reflector, R is less than 0.25; and for a perfect reflector, R equals unity. The minimum is always sharper than the maximum, particularly if the reflection factor is near unity (Figure 5). If the incident and reflected waves are in phase, the sample surface is rigid. If the reflected wave is 180 degrees out of phase with the incident wave, the surface is pressure release. If $0^{o} < \phi < 180^{o}$, the surface is mass-like. If $-180^{o} < \phi < 0^{o}$, the surface is compliant.

Once the reflection factor R has been found, the absorption coefficient is given by:

$$a = 1 - |R|^2 \quad . \qquad (3.16)$$

The experimental value of the impedance at the surface of the sample material can be computed from,

$$\overline{Z} = \xi\rho_0 c_0 \qquad (3.17)$$

where ξ is the normalized impedance given by:

$$\xi = -\left[\frac{\bar{R} + 1}{\bar{R} - 1}\right] \quad , \tag{3.18}$$

and ρ_0 and c_0 are the density and sound speed of water, respectively. According to the relationship between the impedance and the reflection factor, a certain value of $\bar{R}$ belongs to every given value of $\bar{Z}$ and vice versa, and is represented by the equation

$$\bar{R} = \frac{\bar{Z} - \rho_0 c_0}{\bar{Z} + \rho_0 c_0} \quad . \tag{3.19}$$

In the complex Z-plane Equation (3.19) may be shown graphically, where the corresponding values of the absorption coefficient are also given (Figure 7)[20].

CHAPTER IV

EXPERIMENTAL PROCEDURE

4.1 Measurement of Standing Wave Interference Patterns

All measurements were made in the water tank at an ambient room water temperature of approximately 69.8°F(21°C). The instrumentation hookup is shown in Figure 4. The source or projector and the receiver are suspended from the top of the tank. An imaginary horizontal axis is placed between the projector and the receiver at mid-depth in the water tank, and the transducers are mounted slightly off this axis in order to minimize mutual interference. Pulsed sound signals with a pulse length of 0.1 msec were used. On the receiving side, the gate was set at slightly less than 0.1 msec in order to eliminate the leading and trailing edges of the pulse train. The separation distance between the projector and receiver was approximately 36 inches at the beginning of a given scan, but as the receiver moved away from the test sample, the separation decreased to 30 inches. This range was chosen because it resulted in a good signal-to-noise ratio. The measurements were taken in a frequency range of 10 to 50 kHz, in incremental frequency steps of 1 kHz.

When sound waves are directed towards a given test sample, the reflection factor is computed from the ratio of the measured maximum to minimum pressure amplitude at successive extremes (Figure 5). The multimeter makes visible the pressure maxima and minima as the receiver moves away from the surface of the test sample. The digital voltmeter

makes it possible to record accurately these data. The first and second pressure maxima and minima were recorded, but because of the finite diameter of the receiver, the acquisition of data at the surface of the sample was not possible. In order to determine if there was any variation between the first and second pressure maxima, we calculated the ratios of the first pressure maximum to the first pressure minimum, the second pressure maximum to the second pressure minimum, and the first pressure maximum to the second pressure minimum. These pressure ratio data were then used in a computer program to solve for the reflection factor and the phase angle which may be used in defining the absorption characteristics of the sample materials.

The weights of the samples were taken before and after each test, using a Dillon force gauge, to obtain the air-dried and absorbed weights of each test sample. The final weight is needed in order to calculate the density of the test sample and the moisture content (see Appendix). Prior to the standing wave measurements, each sample of wood was left soaking in the water tank for approximately one week. In addition, after measurements were performed on white pine, it was left to soak for another week to see if the absorption properties would be affected. The surface of the sample and the hydrophones were inspected regularly for air bubbles which, when present, cause erroneous readings. It was found that the presence of air bubbles, even in small quantities, had a very noticeable effect on the acoustic properties of the samples.

CHAPTER V

EXPERIMENTAL RESULTS

5.1 Reflection Factor Versus Frequency

Data for the reflection factor were obtained by moving the receiver relative to the sample in order to measure the acoustic pressure amplitudes in the standing wave field as discussed in Section 4.1. A typical result is illustrated in Figure 8 where the sample is a two layered composite (bubble rubber-steel), and the frequency is 22 kHz. The first pressure maximum and the first pressure minimum are clearly visible, and their ratio d can be substituted into Equation (3.11) to yield a reflection factor of 0.74. Lower reflection factors were obtained using the ratio of the second pressure maximum to the second pressure minimum or the ratio of the first pressure maximum to the second pressure minimum, as compared to using the ratio of the first pressure maximum to the first pressure minimum.

Figures 9 through 21 show the measured reflection factors for the composites described in Section 2.3. Unless noted on the figures, all the measurements were obtained with the steel plate as a backing. Figure 9 shows that the steel-bubble rubber composite, which is used as a reference absorber for the other composites, has an overall reflection factor of 0.4 for frequencies above 30 kHz. This means that it has an absorption coefficient equal to 84 percent (see Section 3.1). The bubble rubber-steel composite (Figure 10) has a more nearly constant level of reflection over the entire range of frequencies (R = 0.73).

It displays an absorption coefficient of less than 50 percent. Figure 17, Saper-T, also displays a constant level of reflection over the entire frequency range and its absorption coefficient equals about 75 percent. All of the data for the remaining composites show a great deal of variation with frequency.

The reflection factors for the four-layered composites (wood, Saper-T, steel, bubble rubber) are lower than the three-layered composites (wood, steel, bubble rubber) when compared for the same species of wood. For all the composites, except that of bubble rubber-steel, the reflection factor shows a tendency to increase, then to decrease. This trend repeats itself for white pine (Figure 14).

Some generalizations may be made from this behavior of the frequency response curves for those composites containing wood. In all instances, the wood was three-quarters of an inch thick meaning that the thickness is a quarter and a half wavelength at 20 and 40 kHz, respectively. Bobber [3] points out that the echo reduction (reciprocal of reflection factor) of a non-absorbing material is a minimum at $\lambda/4$ and a maximum at $\lambda/2$. We see from these data for the composites containing wood that the reflection factor peaks at around 20 kHz and usually shows a dramatic decrease near 40 kHz. This behavior seems to imply that woods are somewhat non-absorbing materials. They exhibit characteristics similar to both baffles and windows, as some attenuation does take place as indicated by reflection factors significantly less than unity. This overall reduction in reflection may be attributed to a simple mismatch of the specific acoustic impedances. Also observe that the amount of water absorbed by white pine (Table I where MC is defined in the Appendix) is directly related to its

acoustic absorption characteristics as illustrated when comparing Figures 14 and 15. This has the effect of increasing its specific acoustic impedance.

In summary, it is observed that the composite of bubble rubber-steel reflects the greatest amount of sound over the entire frequency range and the combinations of steel-bubble rubber and Saper-T-steel-bubble rubber absorb the most sound. Also, the four-layered composites show a distinct decrease in the reflection factor as compared to the three-layered composites. As the moisture content of the woods increase, the reflection factor tends to decrease (illustrated for white pine).

5.2 Phase Angle Versus Frequency

The phase angle is obtained from the spatial distribution of the minimum pressure amplitudes in the standing wave field as discussed in Section 4.1. The distance from the surface of the composite to the first or second pressure minimum defines this phase angle [Equation (3.15)]. Figures 22 through 34 show the measured phase shift between the incident and the reflected wave over the 10 to 50 kHz frequency range. Observe that the phase angle decreases with increasing frequency for all composites. In general, there is not much difference in the phase angle as computed using the distance from the surface of the composite to the first pressure minimum or to the second pressure minimum as noted in Figures 23 to 30. On the other hand, the steel-bubble rubber composite (Figure 22) displays a great variation in phase depending upon which distance is used. This, as with the reflection factor data for this particular composite must be treated with caution.

As noted before, the steel plate was primarily used as a backing and consequently has approximately eighty holes, 3/16-inch in diameter, bored throughout its surface area. It is suspected that these holes alter the reflective characteristics of the steel plate compared to one of the same size but unobstructed by an array of holes. For the four-layered composites (Figures 31 to 34), the phase angle using the distance of the second minimum pressure is lower than if the distance of the first pressure minimum is used.

From the figures, we may classify the composites' absorption properties as pressure release, mass-like, rigid, or compliant depending on the sign and range of the angle. Some composites display mass-like qualities at low frequencies and then rapidly approach a compliant surface at higher frequencies. Mass-like properties are displayed by bubble rubber and fir plywood (Figures 23 and 26) over the entire frequency range. The other composites vary dramatically in the classification of their acoustic properties with frequency.

CHAPTER VI

DISCUSSION OF RESULTS

For the application of minimizing acoustic reflectivity due to standing radial waves in the 48 inch test section of the Garfield Thomas Water Tunnel, it is desirable to choose acoustic materials that have high absorption coefficients and high attenuation constants in the frequency range of measurement. In order to obtain maximum transmission and minimum reflection of sound waves passing through the water-to-sample interface, it is also necessary to match the acoustic impedance at the interface. In principle, the reflection factor and the phase angle, alone, will suffice to provide information on the acoustic properties of the sample. These data were obtained experimentally in this investigation. However, the techniques commonly used to determine the sound speed and the attenuation constant in the samples are based on the boundary conditions imposed by the sample and its mounting or backing. Kinsler and Frey [11] explain these techniques for two-layered media which may be extended to the cases of three- and four-layered media. Originally, we assumed that bubble rubber acted as an air or pressure release backing and that the steel plate acted as a rigid backing. With the first assumption, the boundary condition for the samples mounted on the bubble rubber would be that the pressure at the interface vanishes. In the case of the steel backing, the particle velocity at the interface is assumed to vanish. These assumptions greatly simplify the theory. As shown in

Figure 23, the acoustic properties of the bubble rubber-steel is mass-like, contrary to our assumption. A pressure release surface means that all the sound is reflected and that the reflected wave is 180 degrees out of phase with the incident wave. Similarly, all the sound is reflected at a rigid surface, but the reflected wave is in phase with the incident wave. From Figures 9 and 10, observe that neither the bubble rubber nor the steel plate, reflect all of the sound. At low frequencies, the steel plate might be considered rigid. But, for the frequency range of measurement, we observe that the steel plate has a very low reflection factor. In fact, bubble rubber has the highest reflection factor of all the samples investigated, but still absorbs some sound. For these reasons, the classical theories for determining the phase velocity and attenuation per unit length within the sample materials have not been applied in this investigation.

Two factors could contribute to energy loss (absorption) in the bubble rubber. First, bubble rubber is not completely water-tight and absorbs water over a period of time which causes a reduction in the reflection factor (Figure 10). Second, the bond between the bubble rubber and the steel plate is not perfect, causing water to get in between the materials. The screw holes distributed uniformly in the steel plate for purposes of attaching the wooden samples could alter the reflection depending on the diameter of the holes and their spatial distribution. Absorption in the wooden samples is due to an increase in the moisture content which causes an increase in the density, and also influences the compression modulus. These, in turn, increase the specific acoustic impedance. It is suspected that the dramatic variation of their acoustic properties with frequency is also

due to the fact that wood is a non-homogeneous, anisotropic material and is able to support several modes of wave propagation simultaneously. As these various modes interfere with one another, internal constructive interference occurs at some frequencies, while destructive interference occurs at others. Therefore, in computing the impedance of composite layers of a certain thickness, the existence of several wave types travelling through the medium, each with its own damping and velocity of propagation, must be taken into account. In general, the impinging sound wave has a forcing effect on the deformation and compression of the medium through the pressure variations which travel across the medium. Absorption occurs if the deformation or motion produces losses.

The peak to valley phenomena which occur in the frequency response for the reflection factor is also illustrated by Mikeska and Behrens [16], even though they determine the echo reduction ($E = p_i/p_r$) versus frequency. Furthermore, the reflection factor of the composites containing a layer of Saper-T are lower than those without this layer, which can be attributed to the fact the Saper-T is designed to attenuate sound (Figure 17).

CHAPTER VII

SUMMARY, CONCLUSIONS, AND RECOMMENDATIONS

This report has described an experimental investigation of the underwater sound absorption characteristics of various combinations of wood, steel, and rubber. The woods considered were white pine, hemlock, redwood, and fir plywood, all three-quarters of an inch thick. The steel used in the experiment as well as the Saper-T rubber was one-quarter of an inch thick, while the bubble rubber (Rubatex) was three-eighths of an inch thick.

The reflection factor for the various composites was determined in the 10 to 50 kHz frequency range by measuring the standing wave field that is generated close to the sample material by mutual interference of the incident and reflected waves. The ratio of pressure maxima to minima was used in conjunction with a theoretical model to define R, the reflection factor. The distance, in terms of acoustic wavelengths, of the pressure minima from the test sample defined a phase angle which was used to characterize the composites in terms of mass-like, rigid, pressure release, or compliant.

In reviewing the open literature on this subject, we found that there were very few published results on the underwater absorption characteristics of various species of wood. Consequently, the data presented here cannot be compared with any other independently acquired data set. Based on the acoustic data (reflection factor and phase angle) obtained in this experimental investigation for the sample composites evaluated, our findings show that:

1. Lower reflection factors are obtained by using the second pressure maximum and minimum to calculate R.

2. The phase angle decreases with increasing frequency for all composites evaluated.

3. The steel-bubble rubber composite has the lowest reflection factor and displays erratic variation in its phase angle with respect to frequency. This behavior may be due to the many holes bored in the steel plate.

4. The bubble rubber-steel composite displays the highest reflection factor and, based on its phase angle, appears to have mass-like properties over the entire range of frequencies.

5. As the moisture content of the wood samples increases, the reflection factor tends to decrease.

6. The composites have lower reflection factors with a layer of Saper-T rubber than without.

7. The experimental data are strongly influenced by air bubbles in the tank, on the samples, or on the transducers. Those data presented were for conditions in which air bubbles were not visibly present.

8. The results depended on the placement of the wooden panels relative to the incoming sound wave. The most repeatable results were obtained when the incident wave insonified a region free of surface irregularities such as knots or the finite cracks that are present between adjacent panels.

This investigation has resulted in some new, but limited, fundamental data on the acoustic reflection characteristics of specific

types of composites. The thicknesses of the various materials used to make up a given composite were not varied, primarily because of the motivation of this study. If an acoustic liner is to be made for the 48-inch diameter Water Tunnel, it seems appropriate to consider materials of commercially standard sizes; thus restricting the thicknesses to those evaluated. However, based on these results, it is questionable as to whether the boundary condition imposed by the tunnel walls has been accurately modeled. The quarter-inch thick steel plate backed by bubble rubber used in this investigation was originally assumed to model the tunnel walls with air on the outside, but the data obtained suggest that this assumption is in error. The tunnel test section is 4-inch thick bronze. We assumed it, as well as the steel plate to be rigid. The steel plate, unfortunately was found to be non-rigid in the frequency range of measurement, so interpretation of these data in terms of absolute values expected for the Water Tunnel should not be attempted. Within the limits of linear acoustics, however, it is reasonable to interpret the results on a relative basis.

The composites containing wood appear not to have smooth frequency responses; they are resonant absorbers. Perhaps the exception to this statement is that composite containing fir plywood (Figure 13). Saper-T rubber also exhibits a rather smooth frequency response (Figure 17), and its reflection factors are slightly less than those of fir plywood. Because of the ease in which Saper-T could be installed in the Tunnel test section, and the fact that it is only a quarter-inch thick leads us to conclude that it would be the most suitable material for a semi-anechoic Water Tunnel liner based on these experimental results. It is

recommended, though, that other commercially available underwater sound absorbing rubbers be evaluated prior to any final decision regarding the material for this liner. If additional work is planned for woods, then it is recommended that the tests be performed within the Tunnel test section itself to assure an accurate modeling of the boundary conditions.

TABLE I

Air-Dried and Water Saturated Densities of Various Species of Wood and Their Moisture Contents

Materials	Air-Dry Density (kg/m^3)	Water Saturated Density (kg/m^3)	Moisture Content (%)
Hemlock	495.16	839.39	70%
Fir Plywood	474.00	829.00	75%
White Pine	429.63	644.14	49 to 56%*
Redwood	324.20	461.38	42%

*two weeks saturated

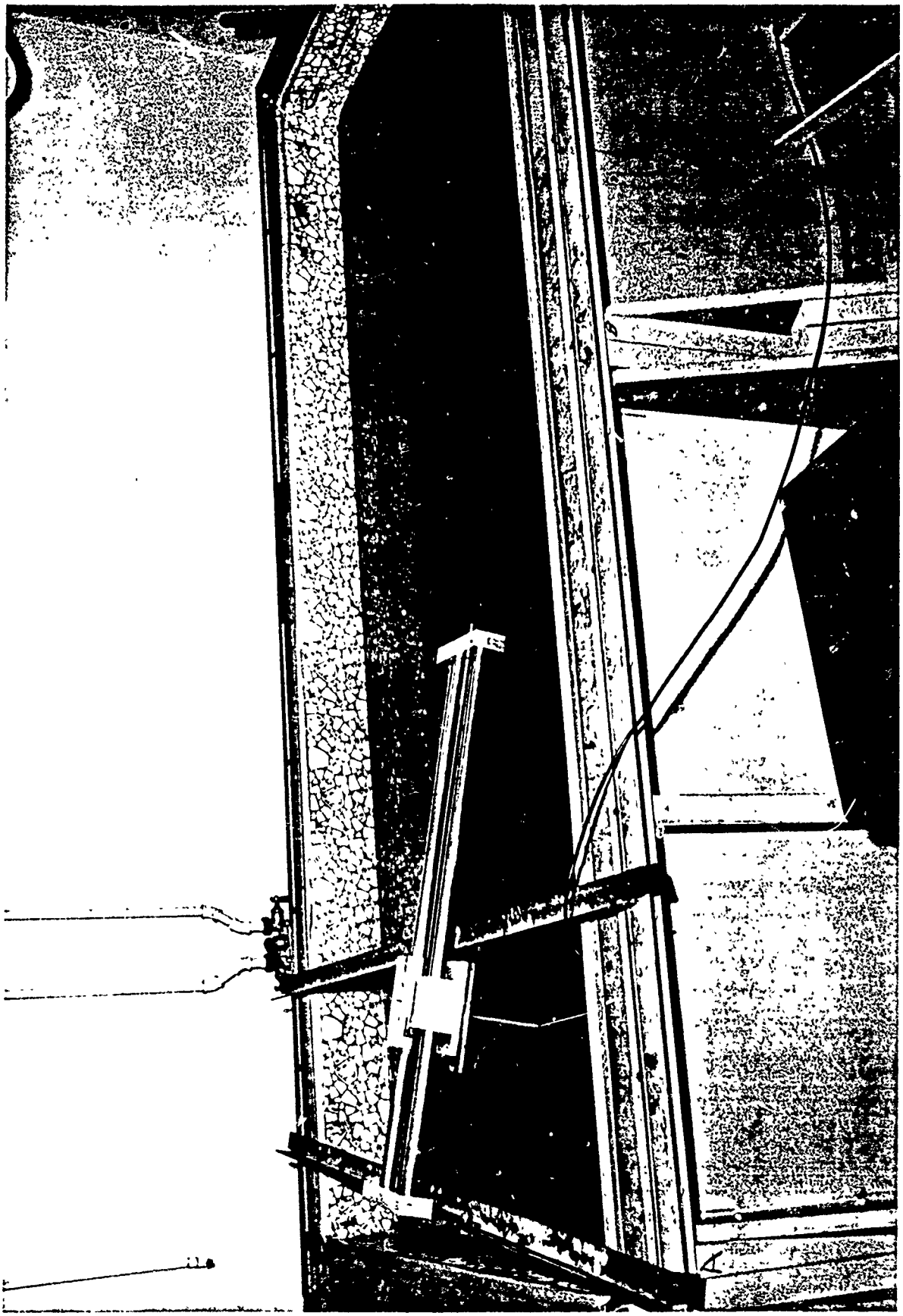

Figure 1. Water Tank (Before Installation of Polyethylene Liner).

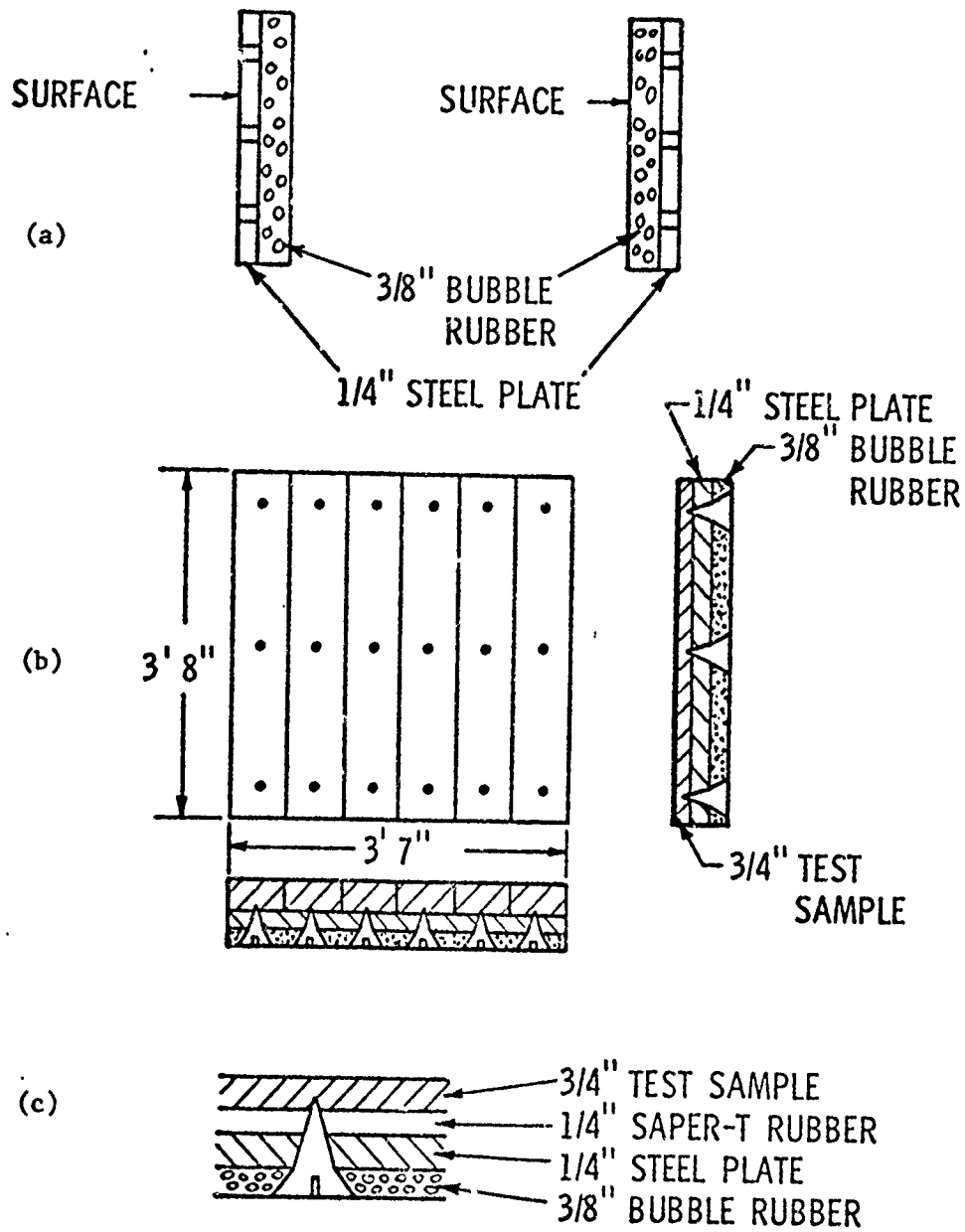

Figure 2. (a) Two-Layered Composites, (b) Three-Layered Composites, (c) Four-Layered Composites.

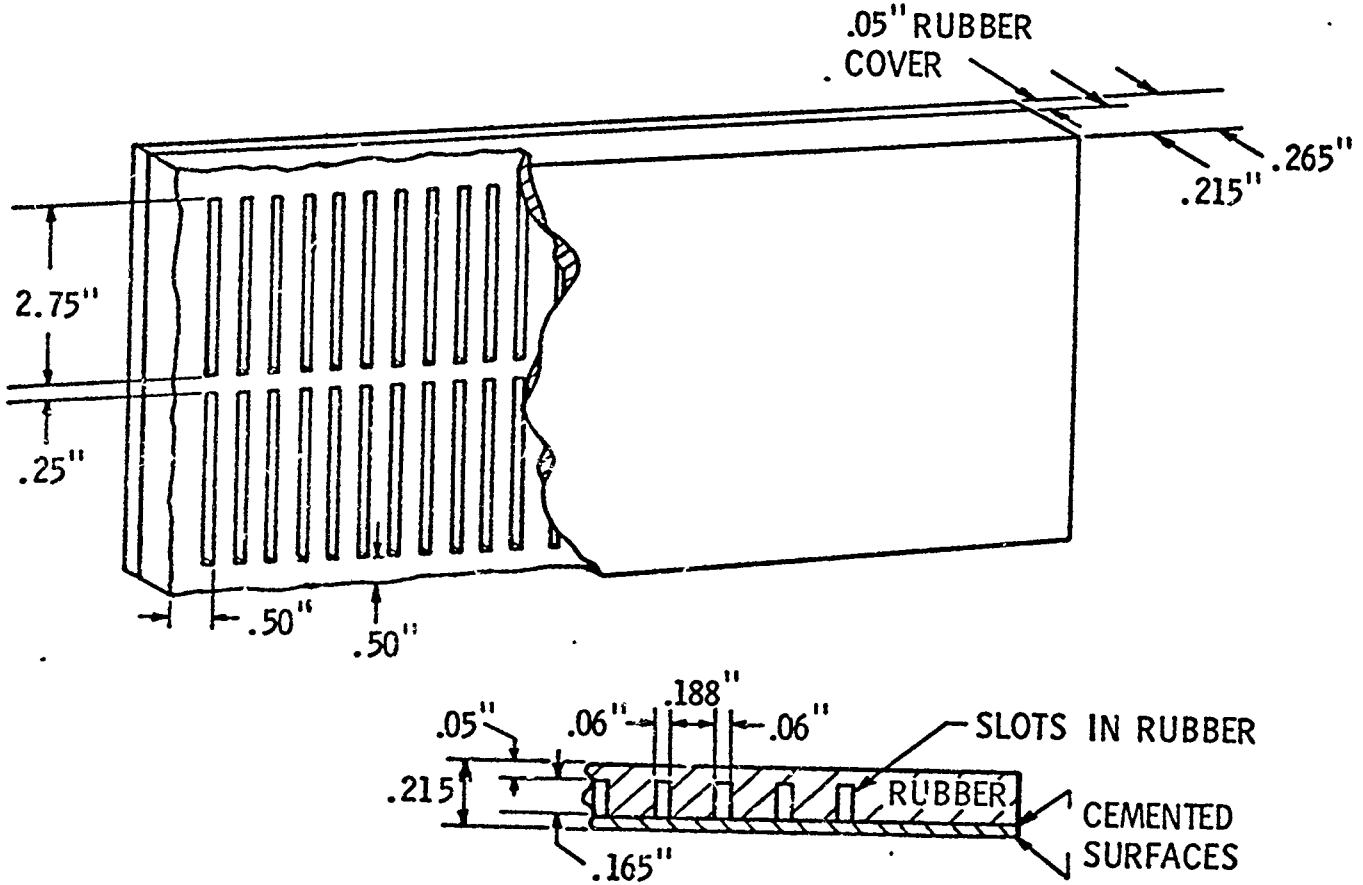

Figure 3. Geometric Configuration of Saper-T Rubber.

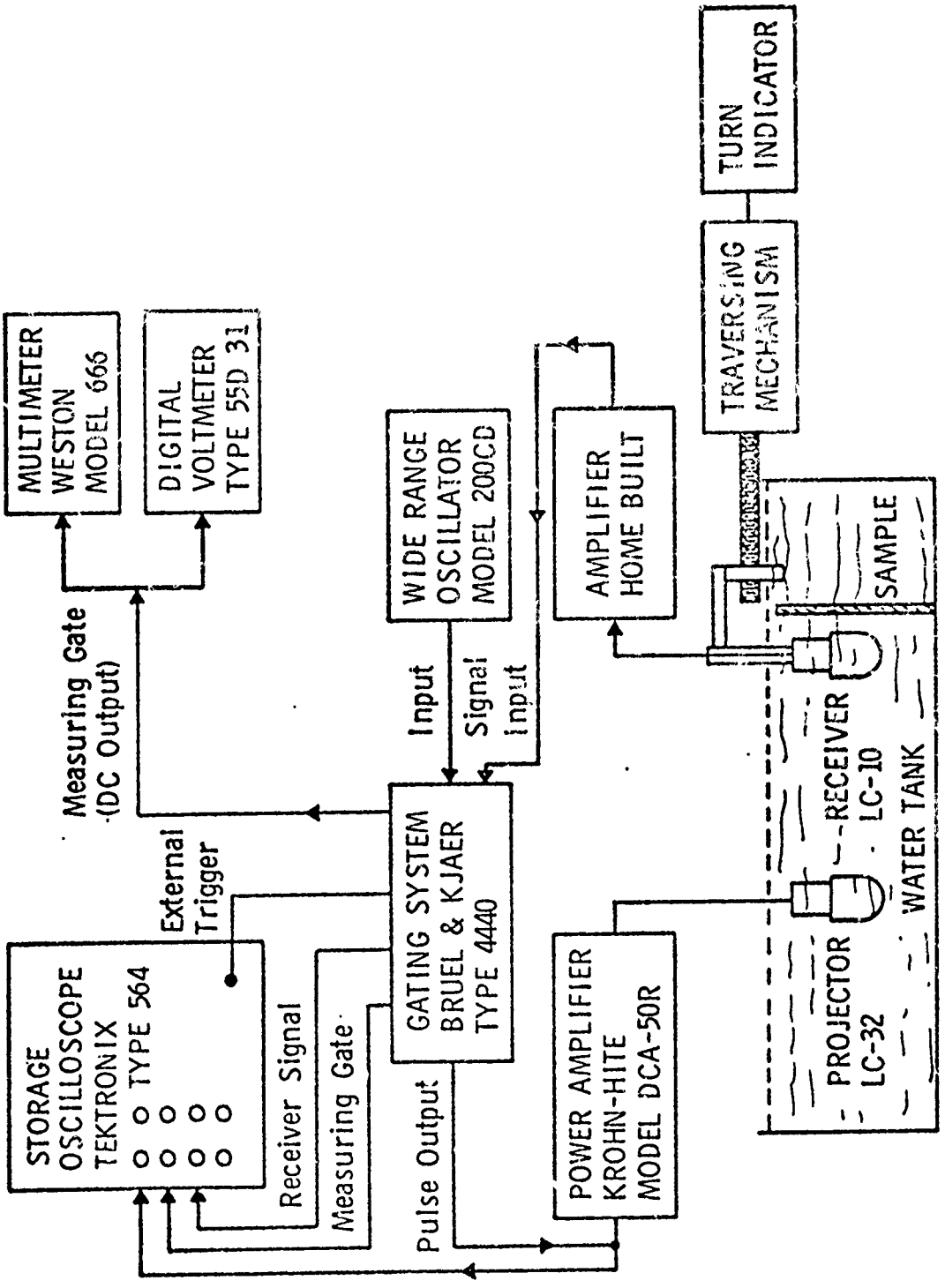

Figure 4. Block Diagram of Instrumentation.

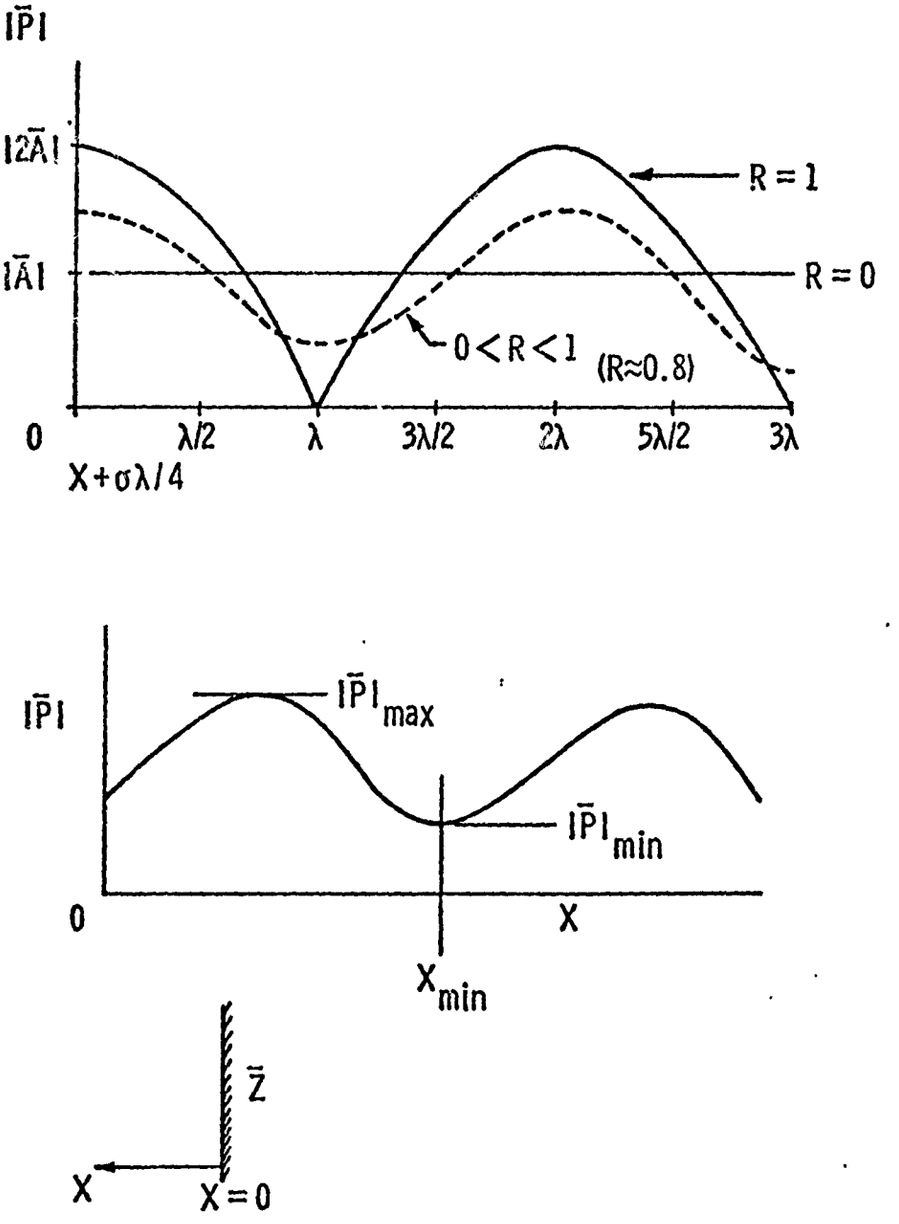

Figure 5. Magnitude of Pressure Versus Displacement for Standing Wave.

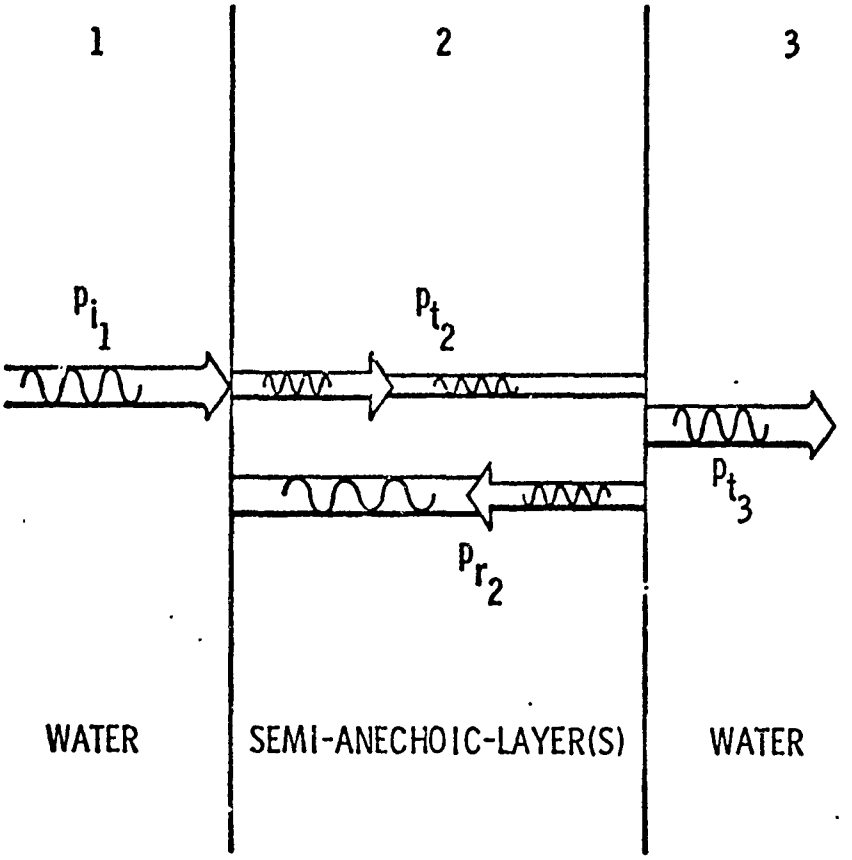

Figure 6. Transmission of Plane Waves Across Semi-Anechoic Layer.

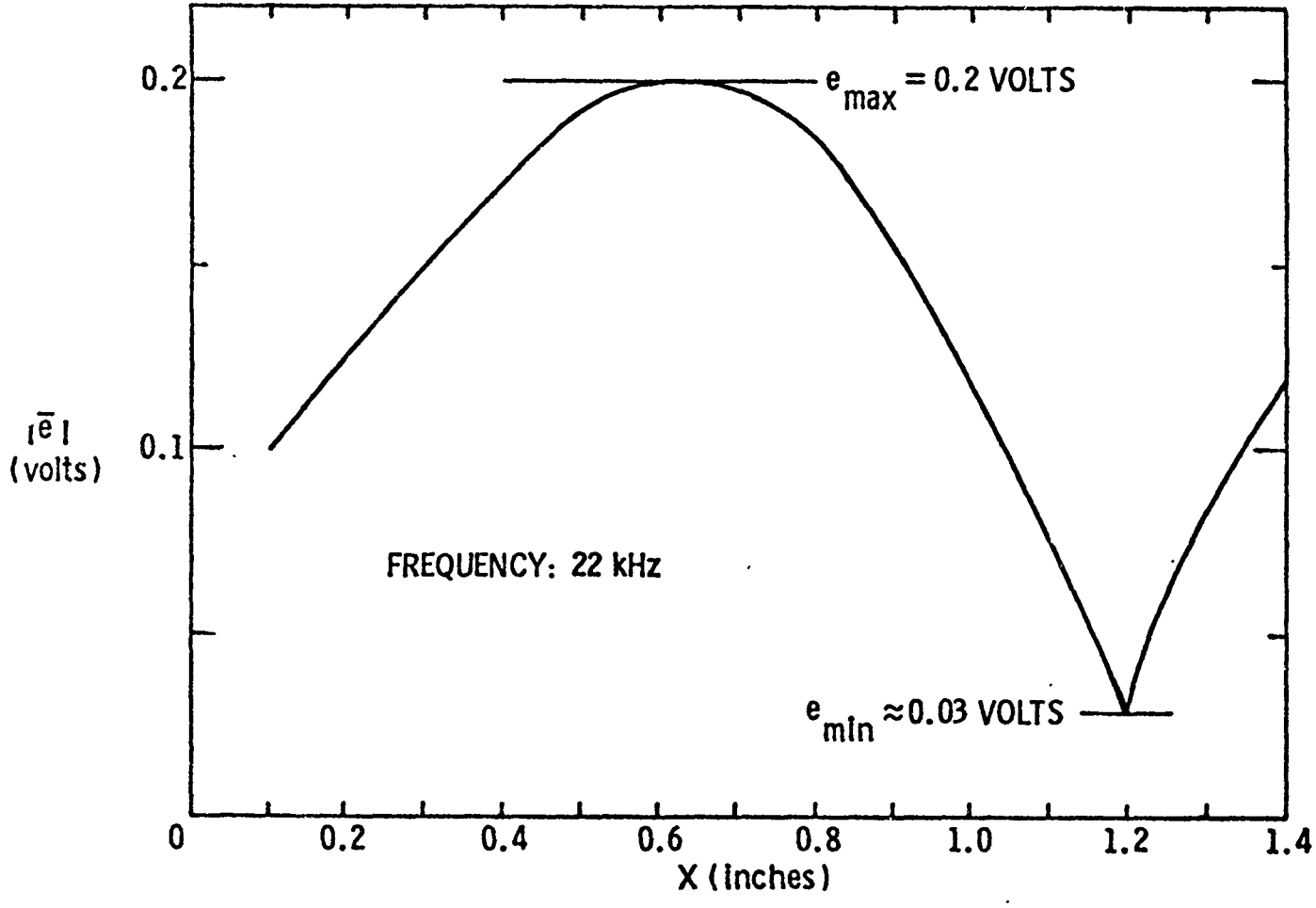

Figure 8. Magnitude of Pressure Versus Displacement for Standing Wave for Bubble Rubber-Steel Composite at 22 kHz.

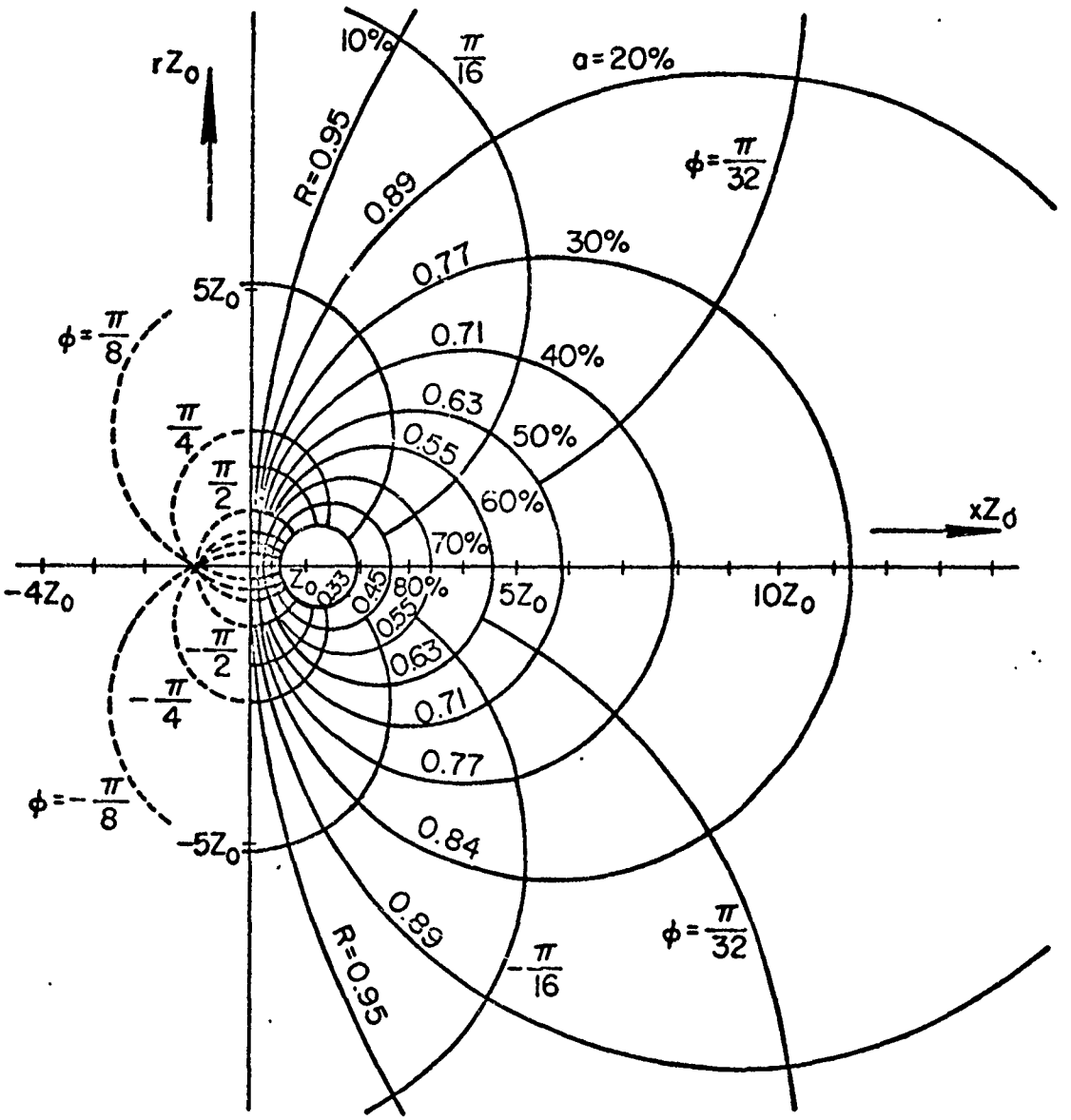

Figure 7. Representation of the Equation $R = (Z - \rho_0 c_0)/(Z + \rho_0 c_0)$ in the Complex Z-Plane.

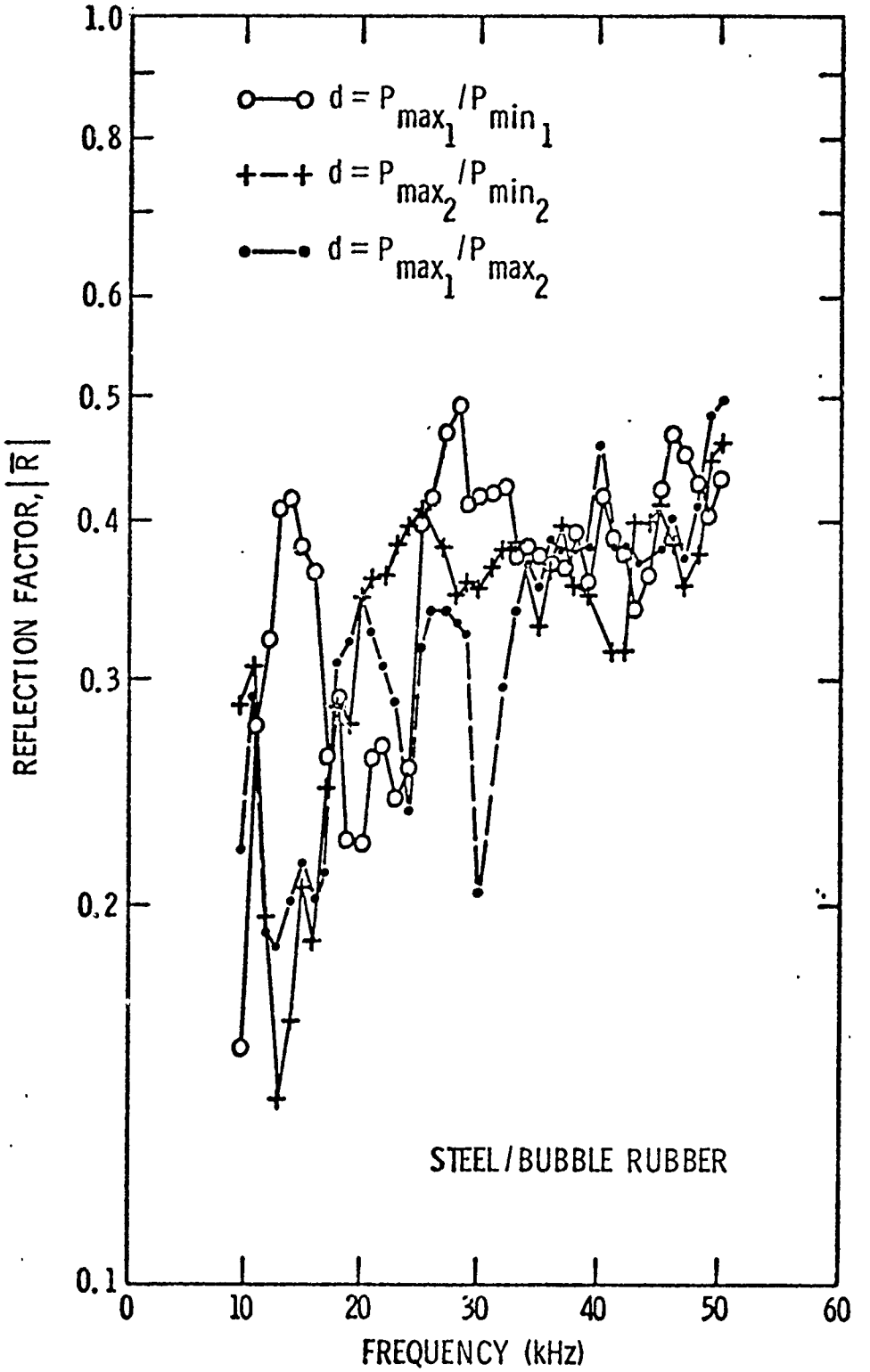

Figure 9. Reflection Factor Versus Frequency for Steel-Bubble Rubber.

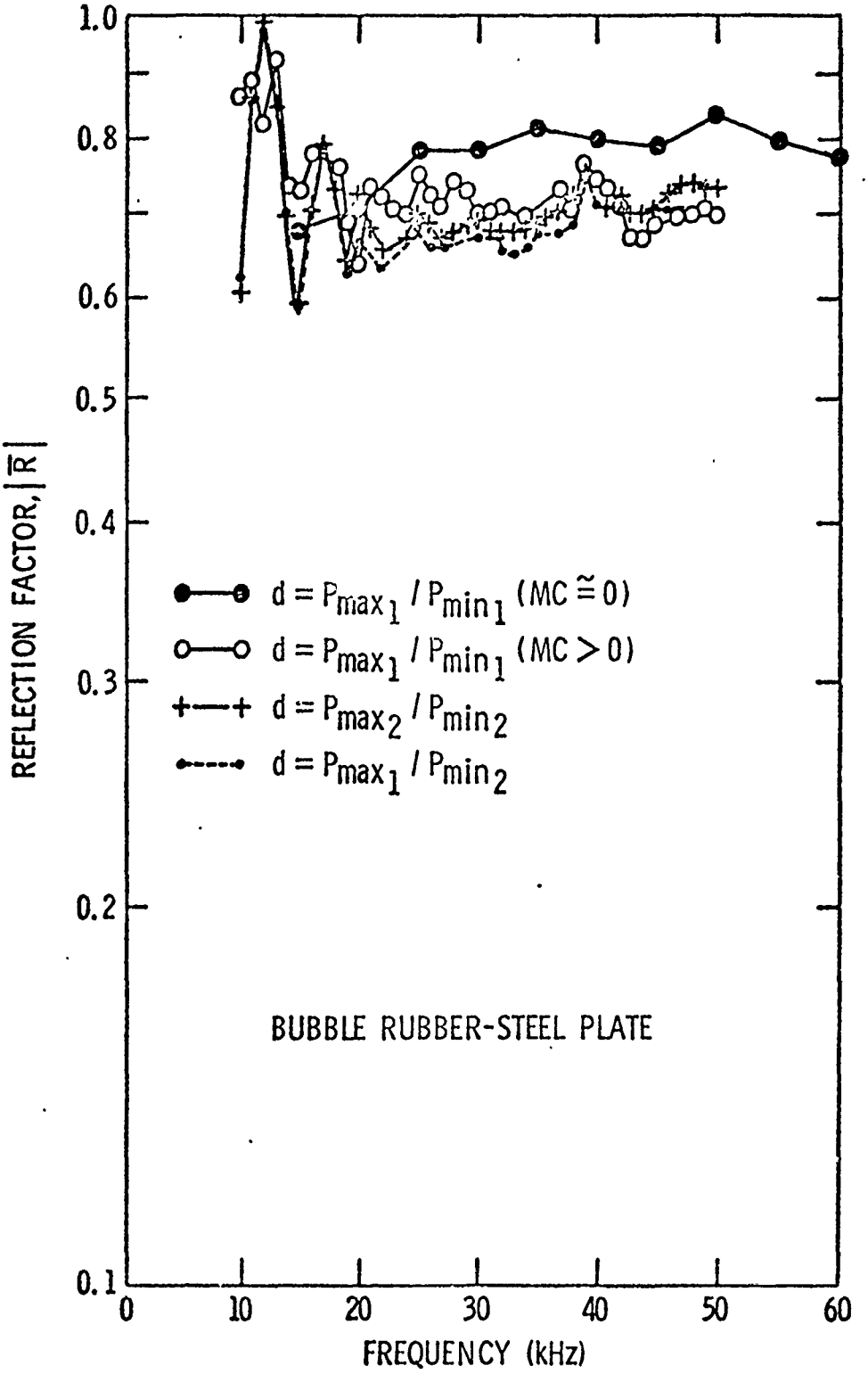

Figure 10. Reflection Factor Versus Frequency for Bubble Rubber-Steel.

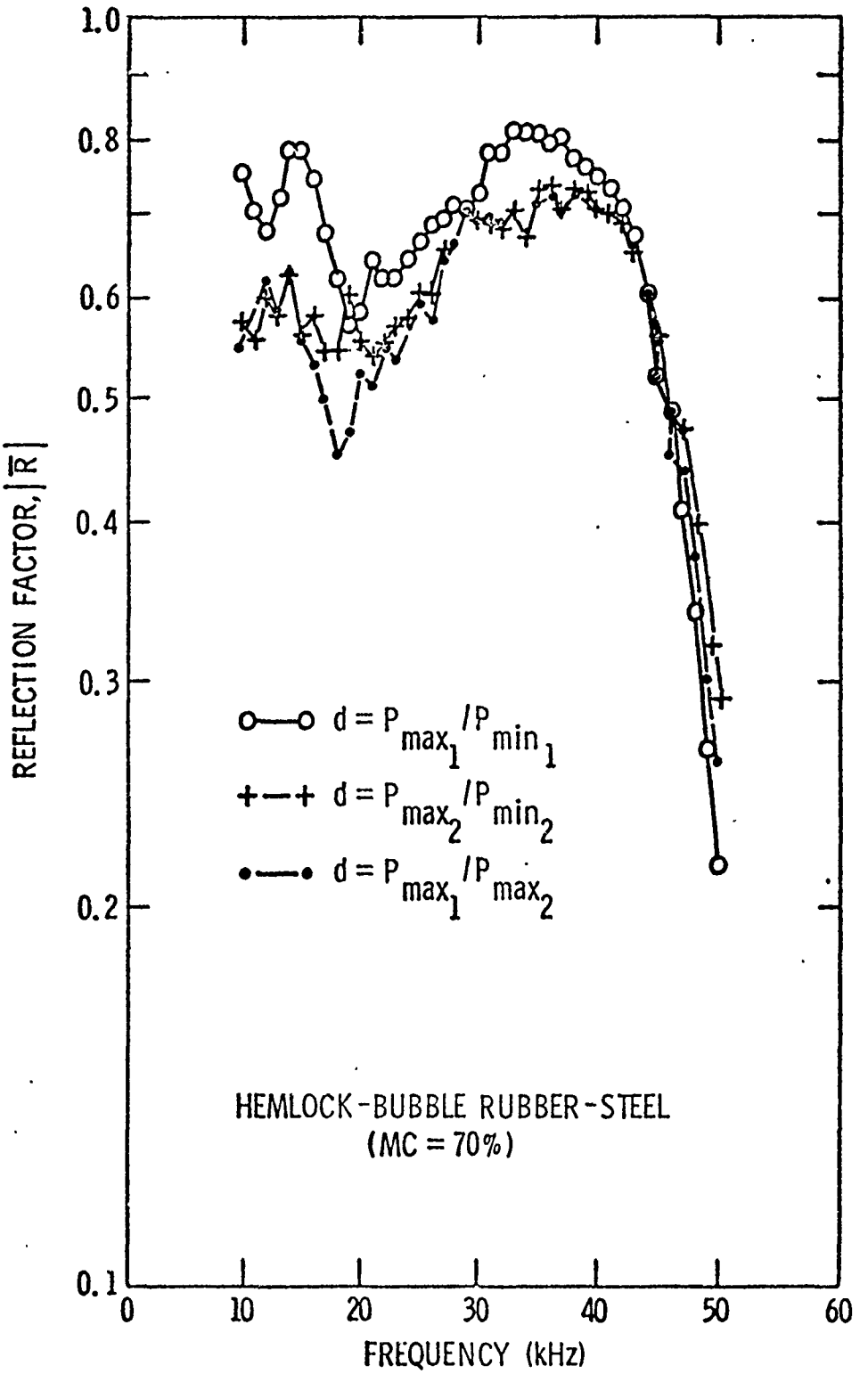

Figure 11. Reflection Factor Versus Frequency for Hemlock-Bubble Rubber-Steel.

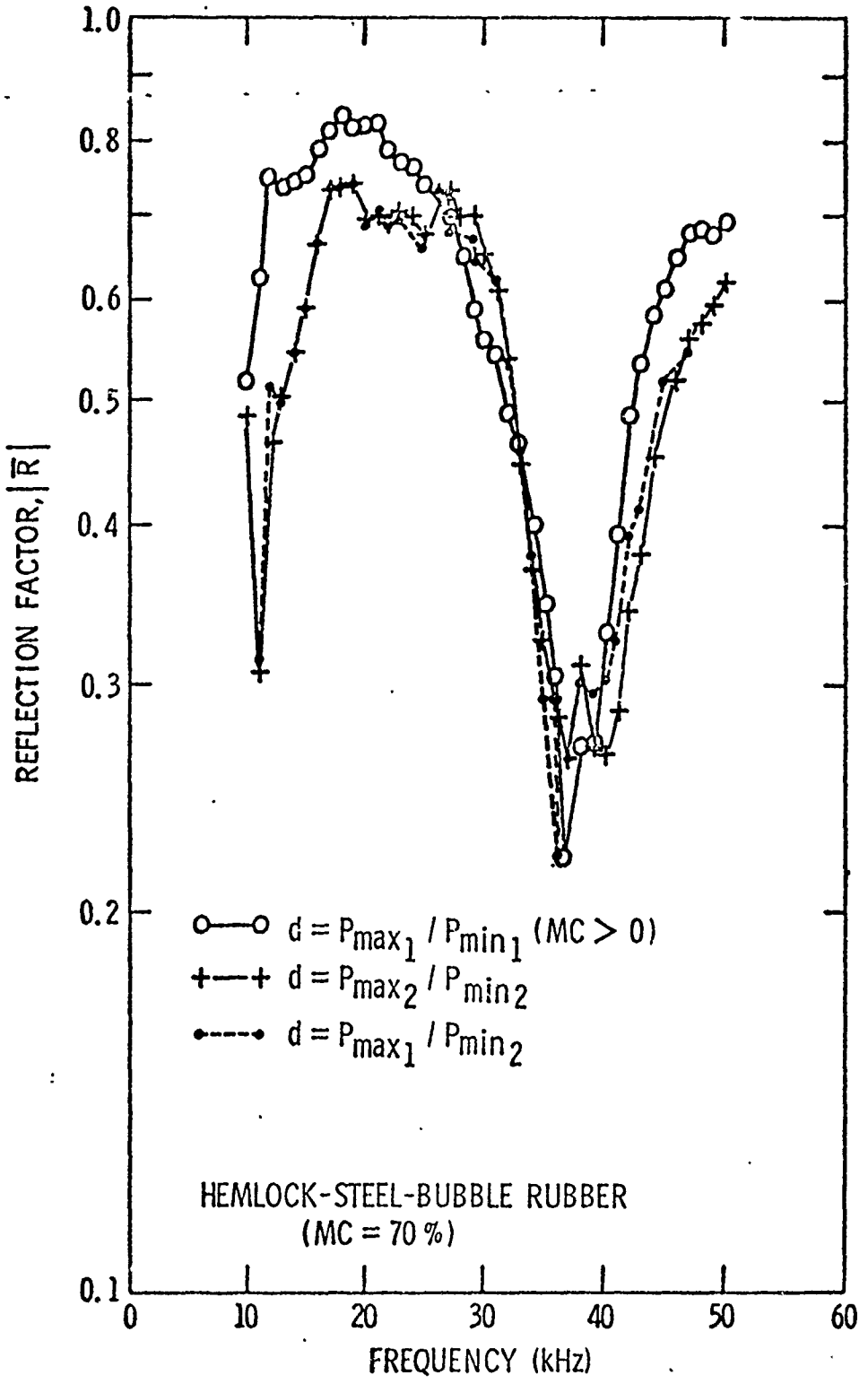

Figure 12. Reflection Factor Versus Frequency for Hemlock-Steel-Bubble Rubber.

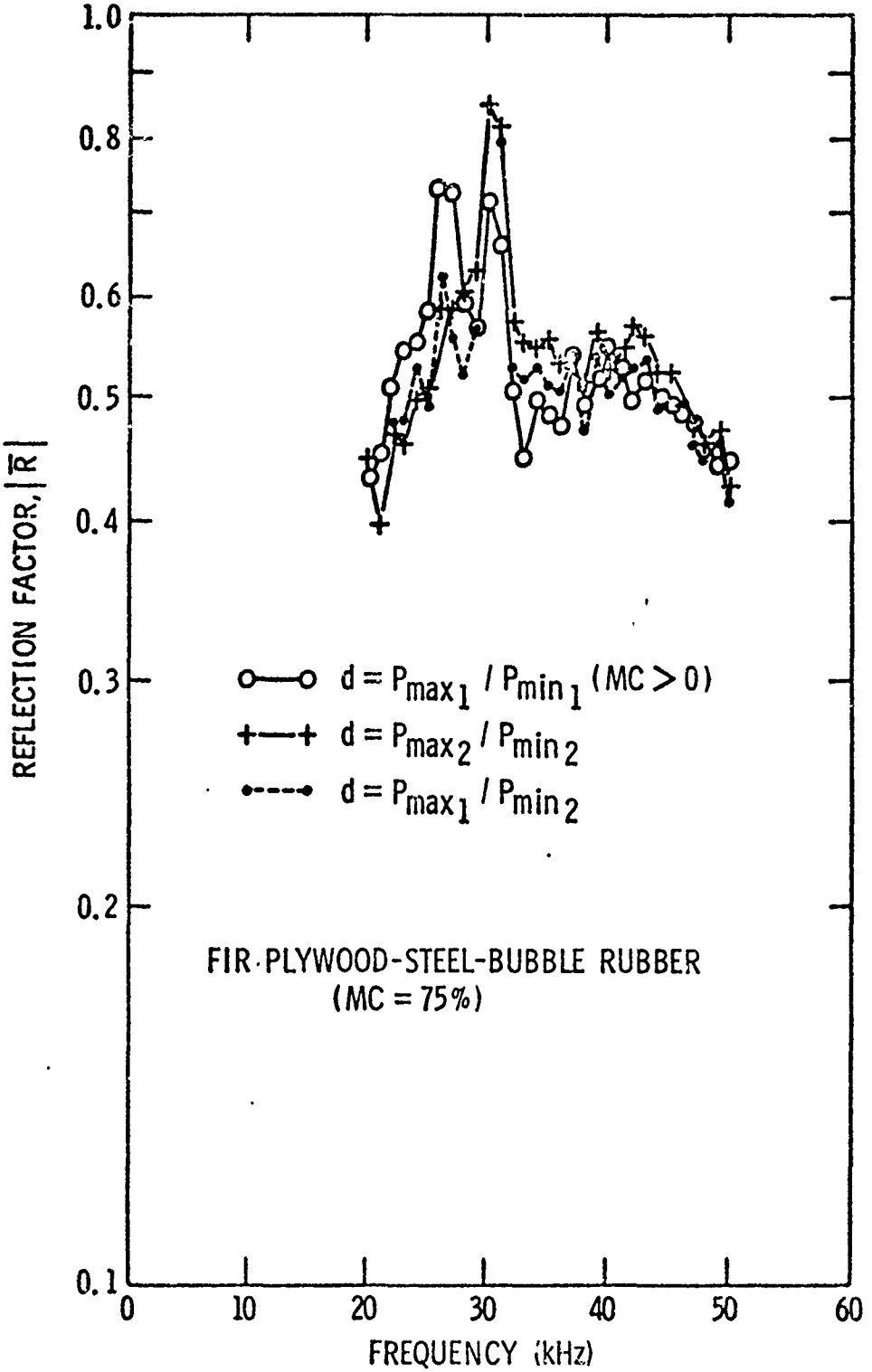

Figure 13. Reflection Factor Versus Frequency for Fir Plywood-Steel-Bubble Rubber.

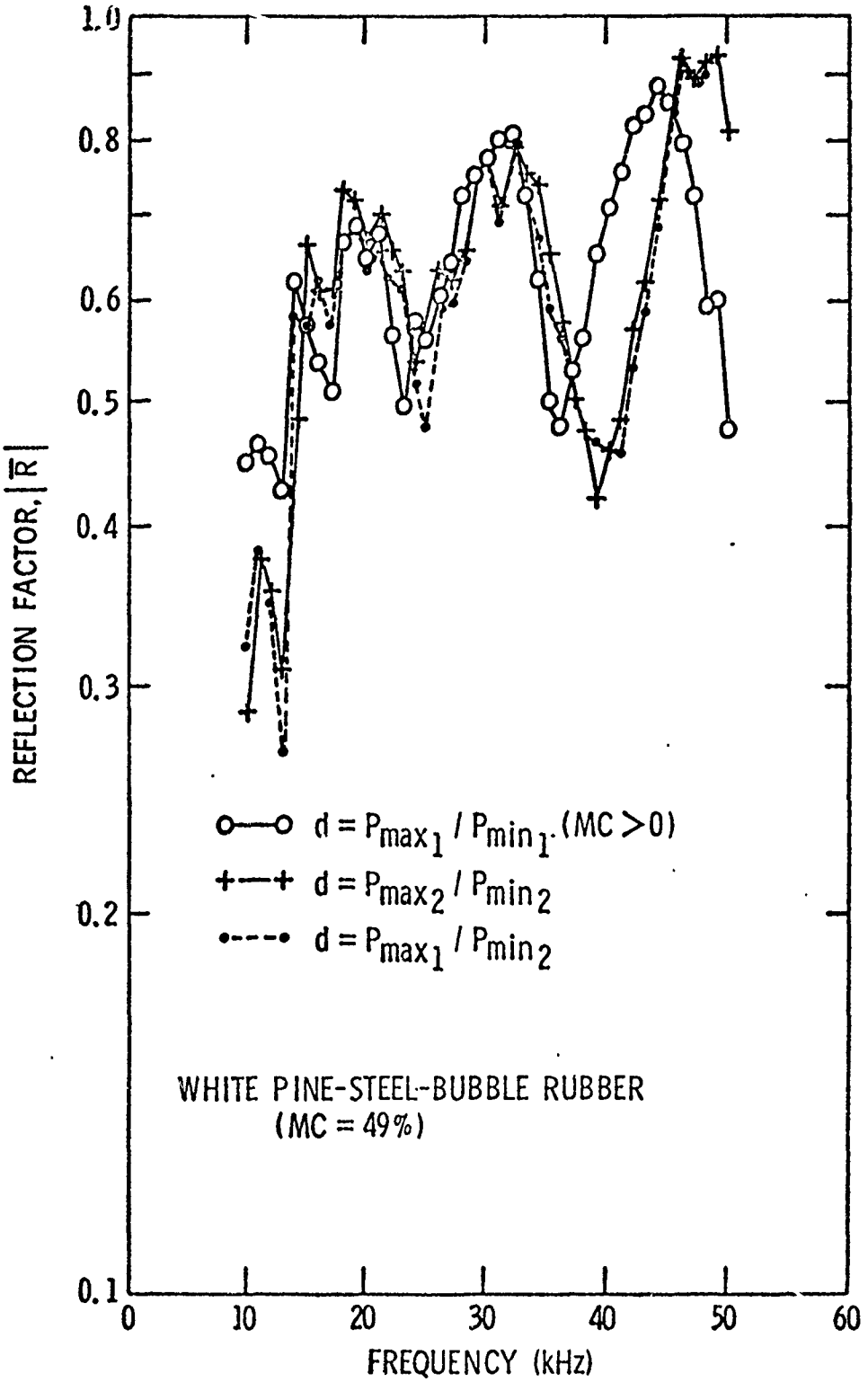

Figure 14. Reflection Factor Versus Frequency for White Pine (49 Percent)-Steel-Bubble Rubber.

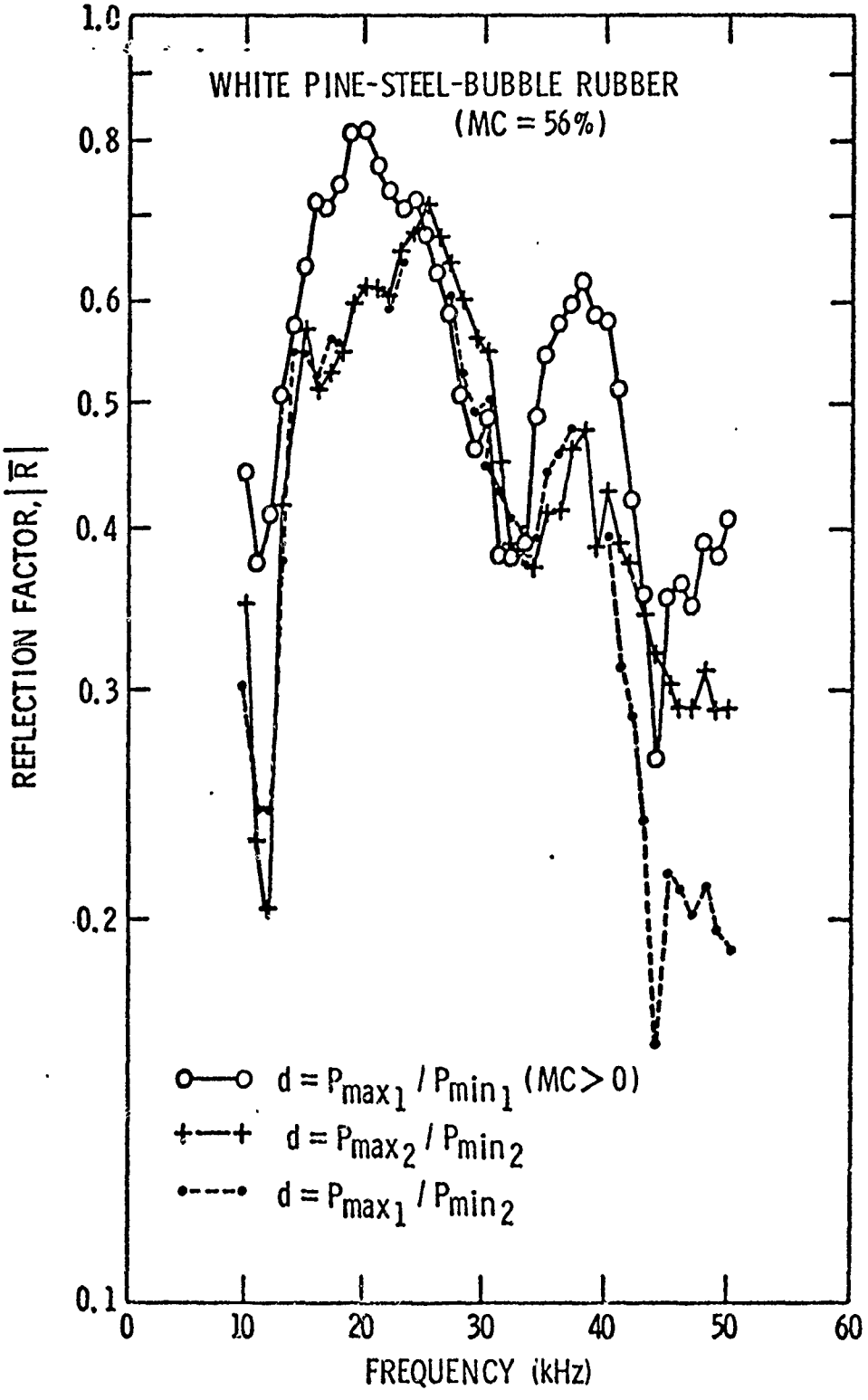

Figure 15. Reflection Factor Versus Frequency for White Pine (56 Percent)-Steel-Bubble Rubber.

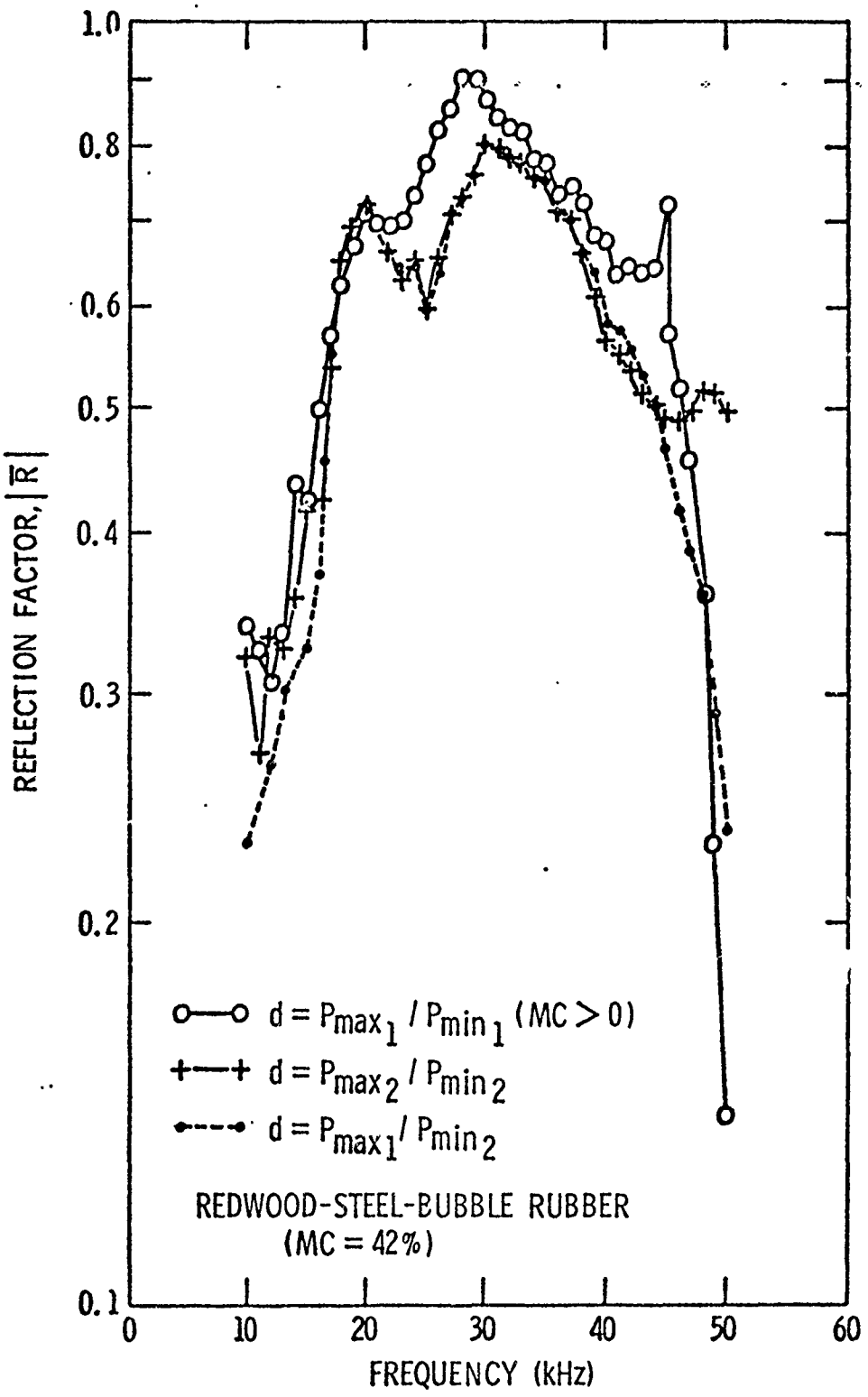

Figure 16. Reflection Factor Versus Frequency for Redwood-Steel-Bubble Rubber.

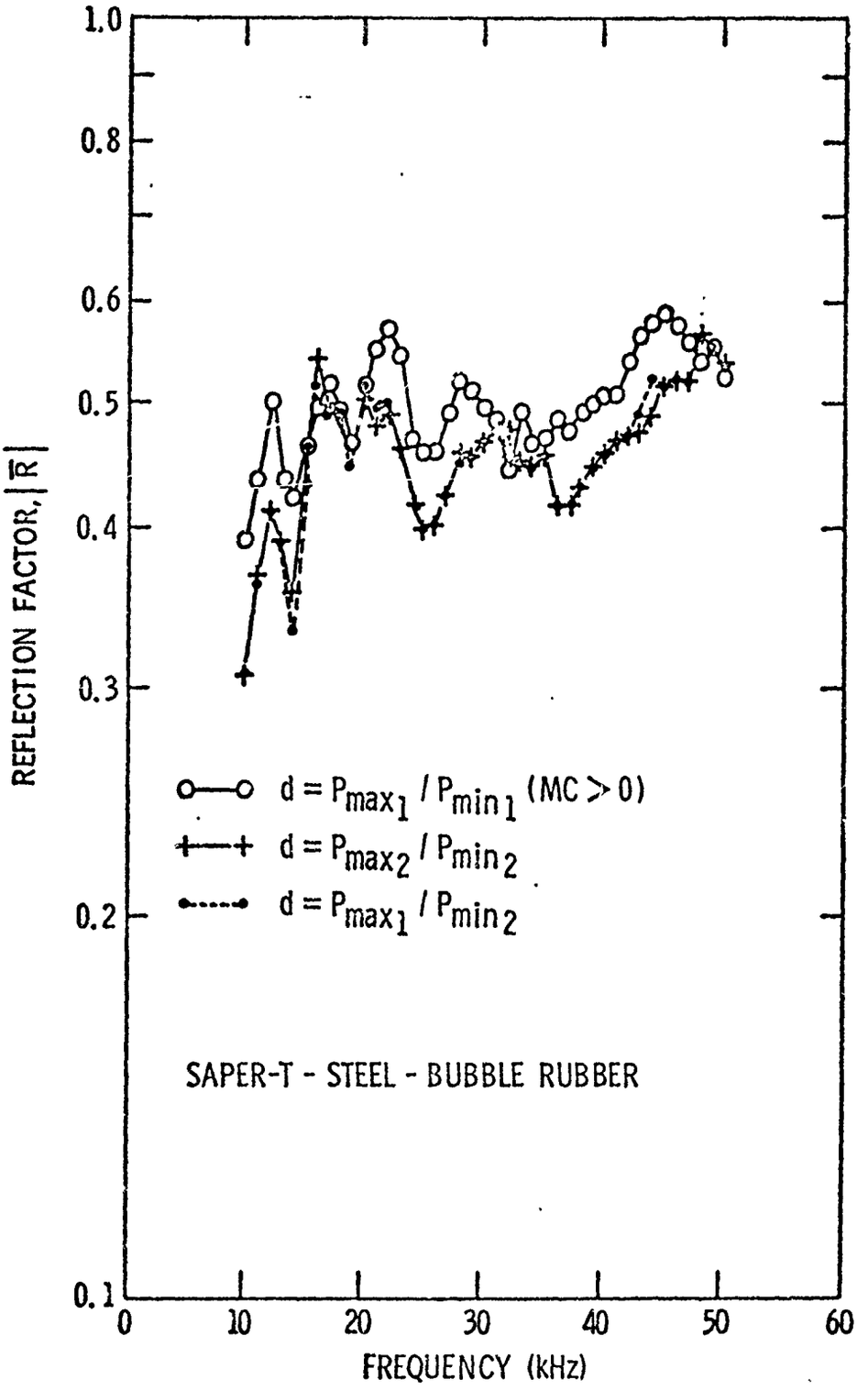

Figure 17. Reflection Factor Versus Frequency for Saper-T-Steel-Bubble Rubber.

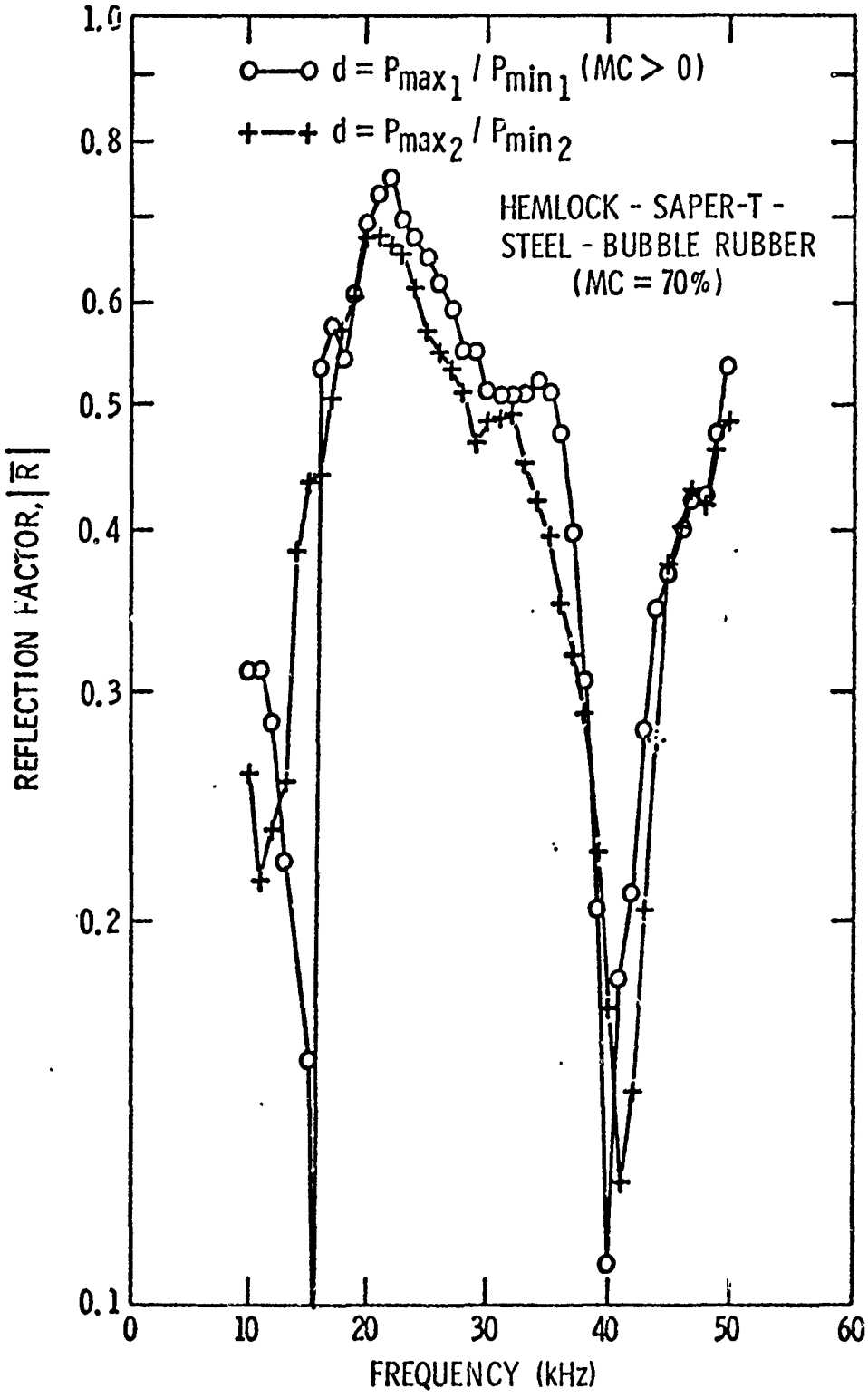

Figure 18. Reflection Factor Versus Frequency for Hemlock-Saper-T-Steel-Bubble Rubber.

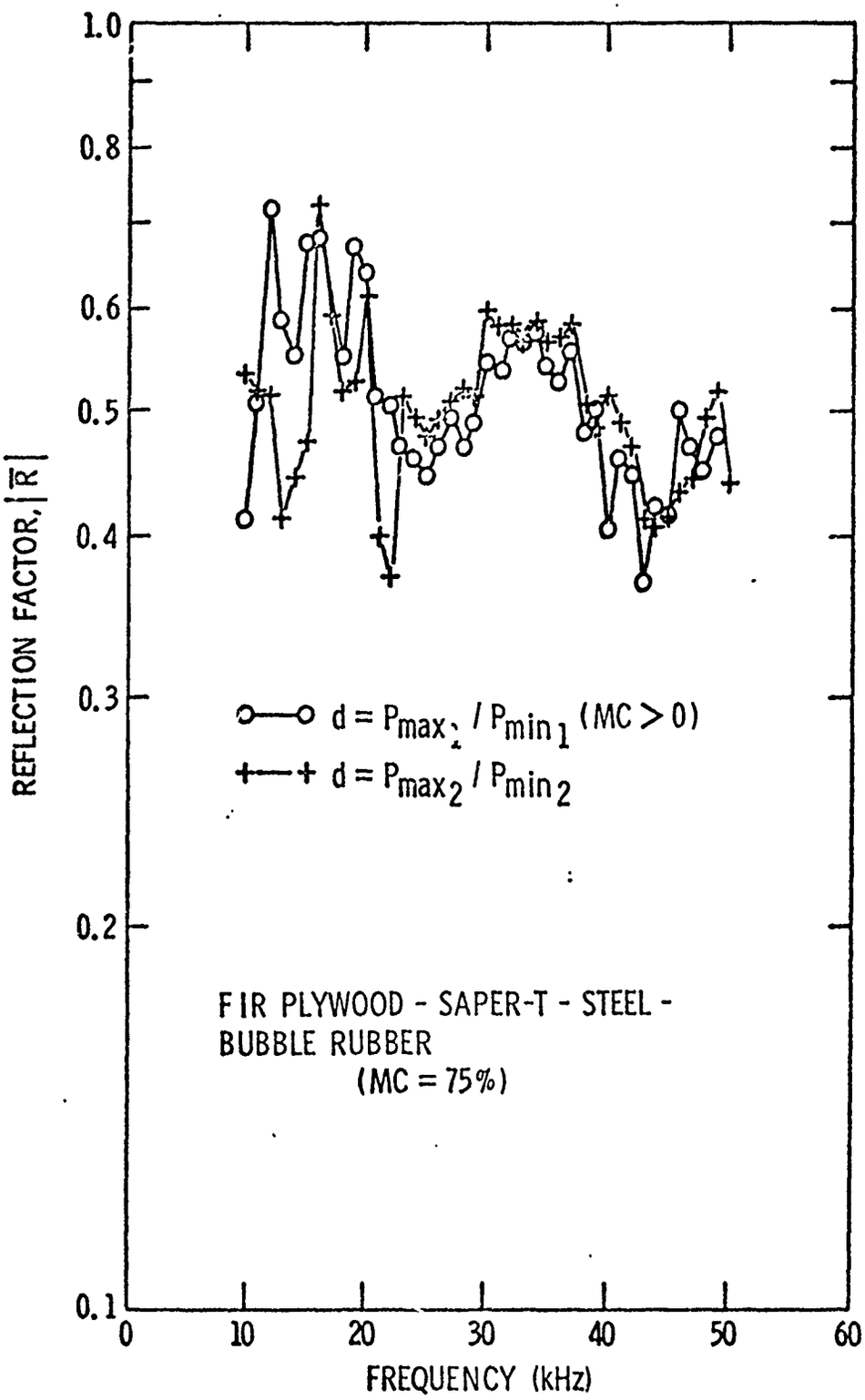

Figure 19. Reflection Factor Versus Frequency for Fir Plywood-Saper-T-Steel-Bubble Rubber.

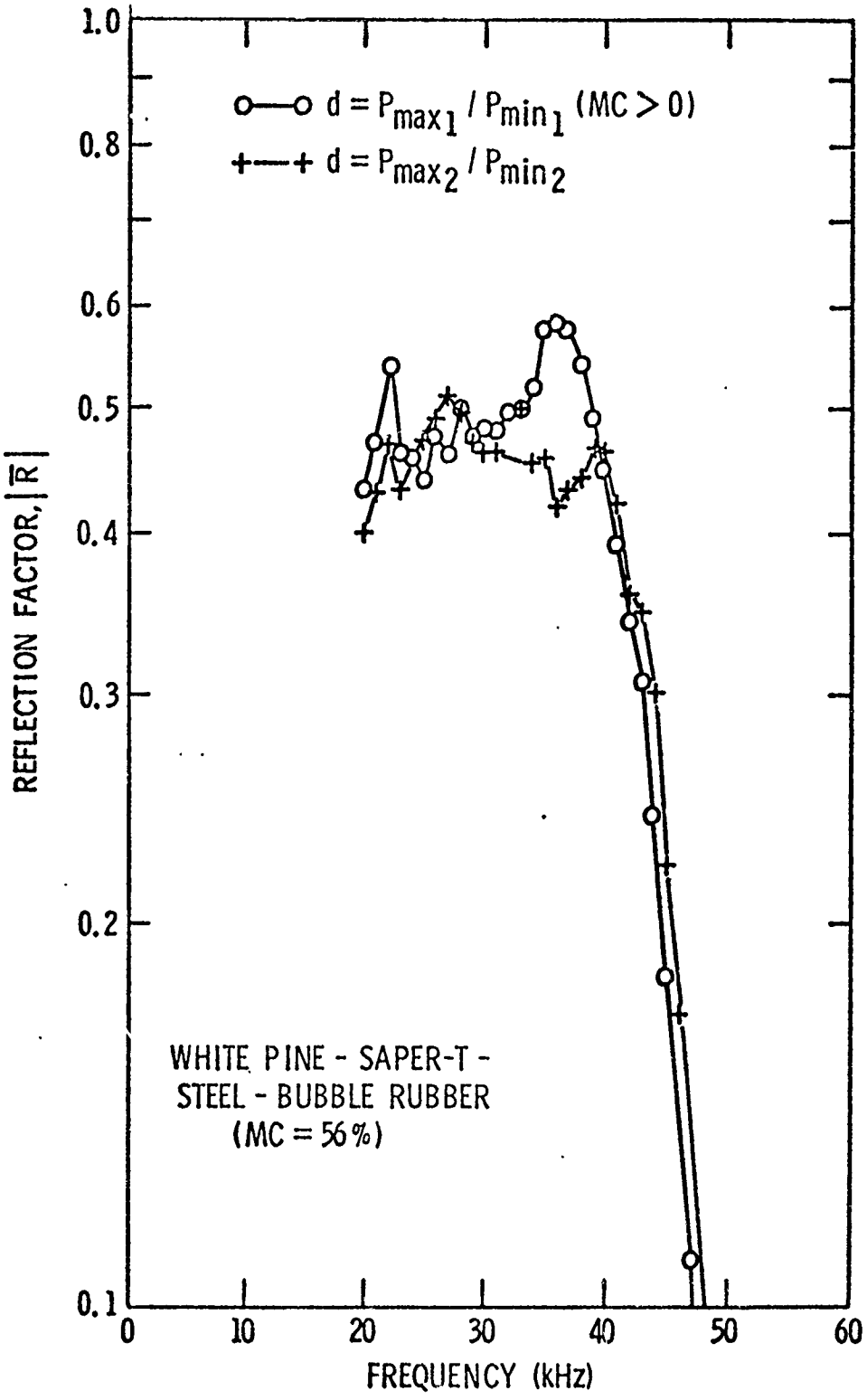

Figure 20. Reflection Factor Versus Frequency for White Pine-Saper-T-Steel-Bubble Rubber.

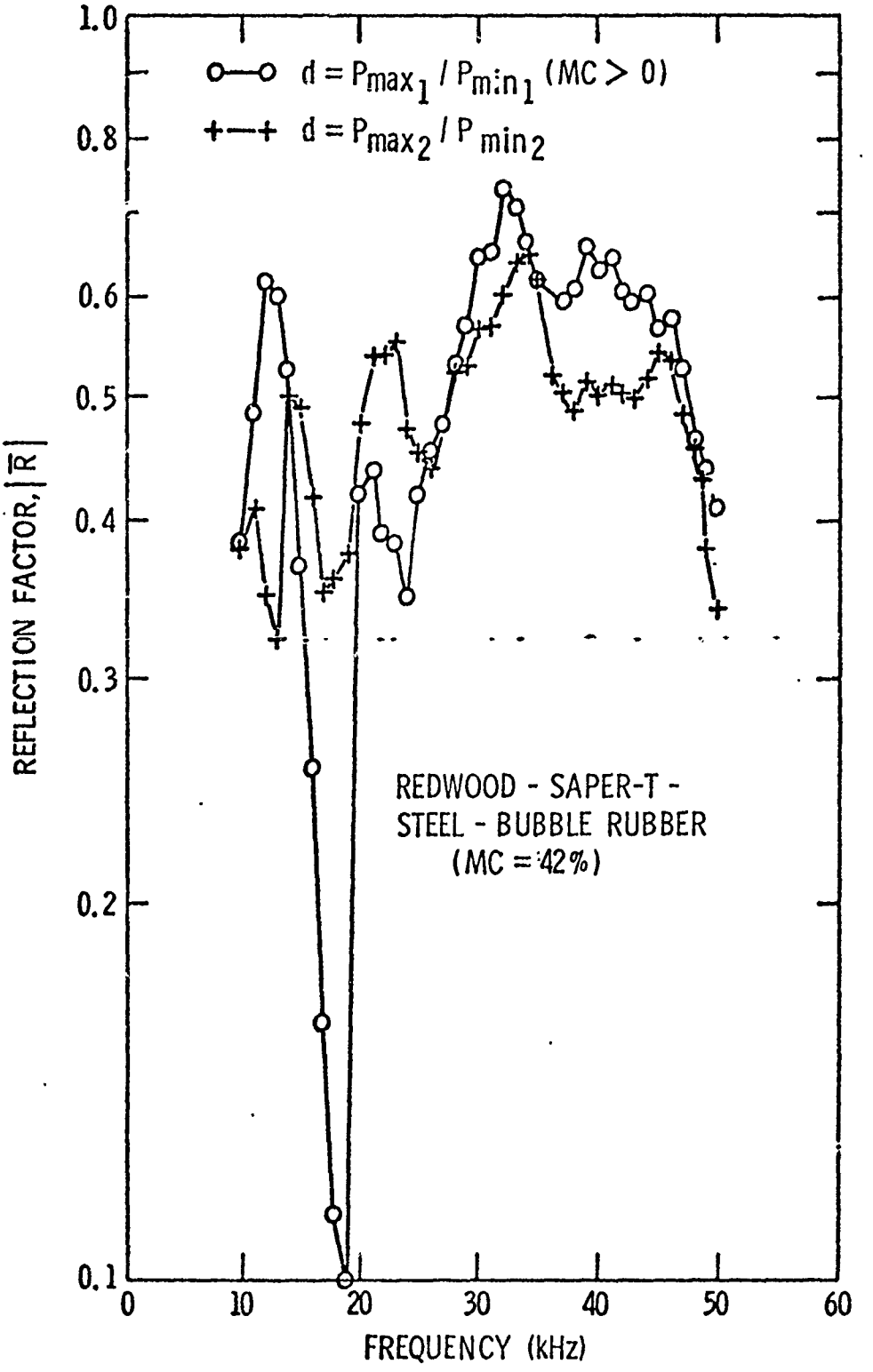

Figure 21. Reflection Factor Versus Frequency for Redwood-Saper-T-Steel-Bubble Rubber.

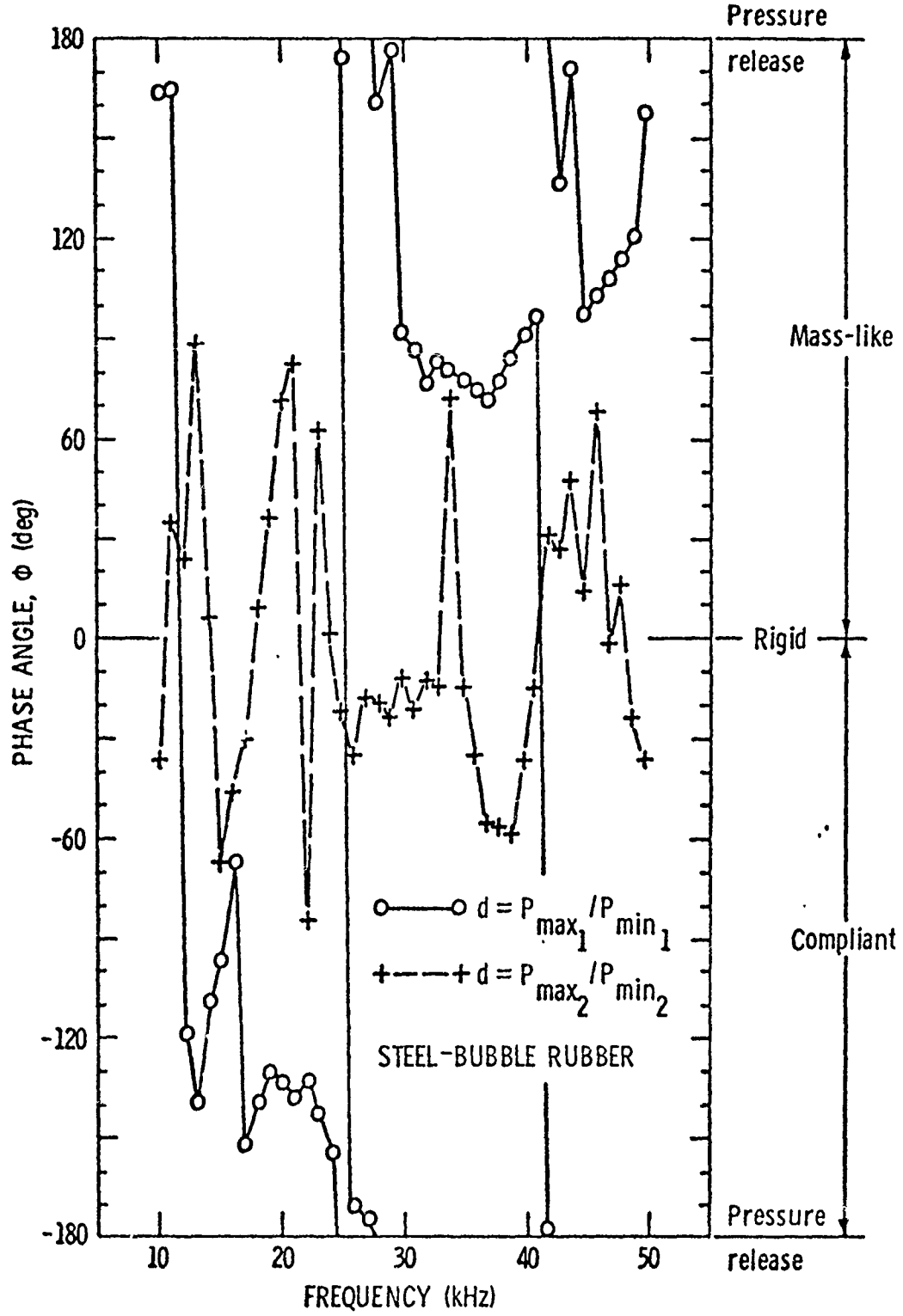

Figure 22. Phase Angle Versus Frequency for Steel-Bubble Rubber.

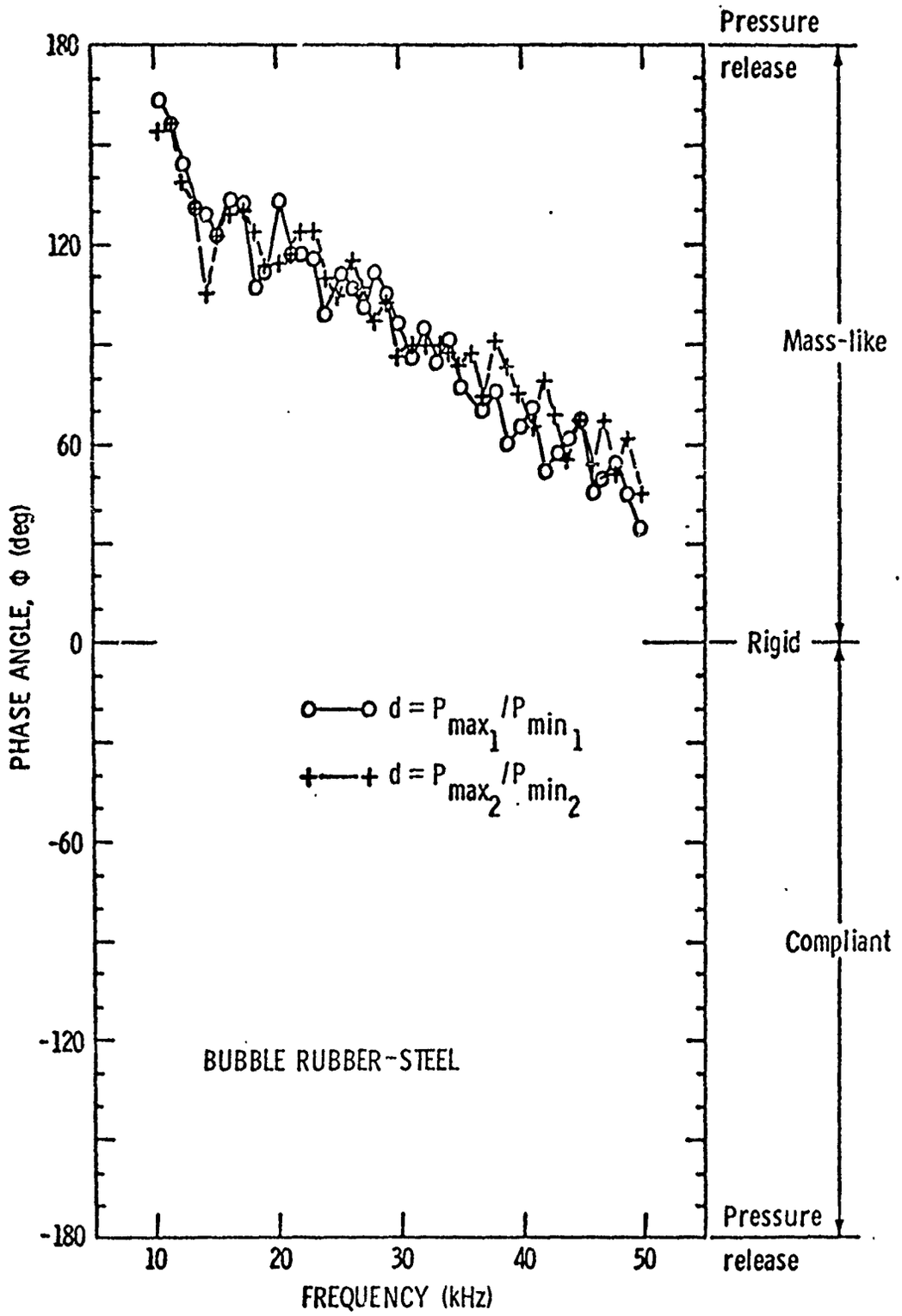

Figure 23. Phase Angle Versus Frequency for Bubble Rubber-Steel.

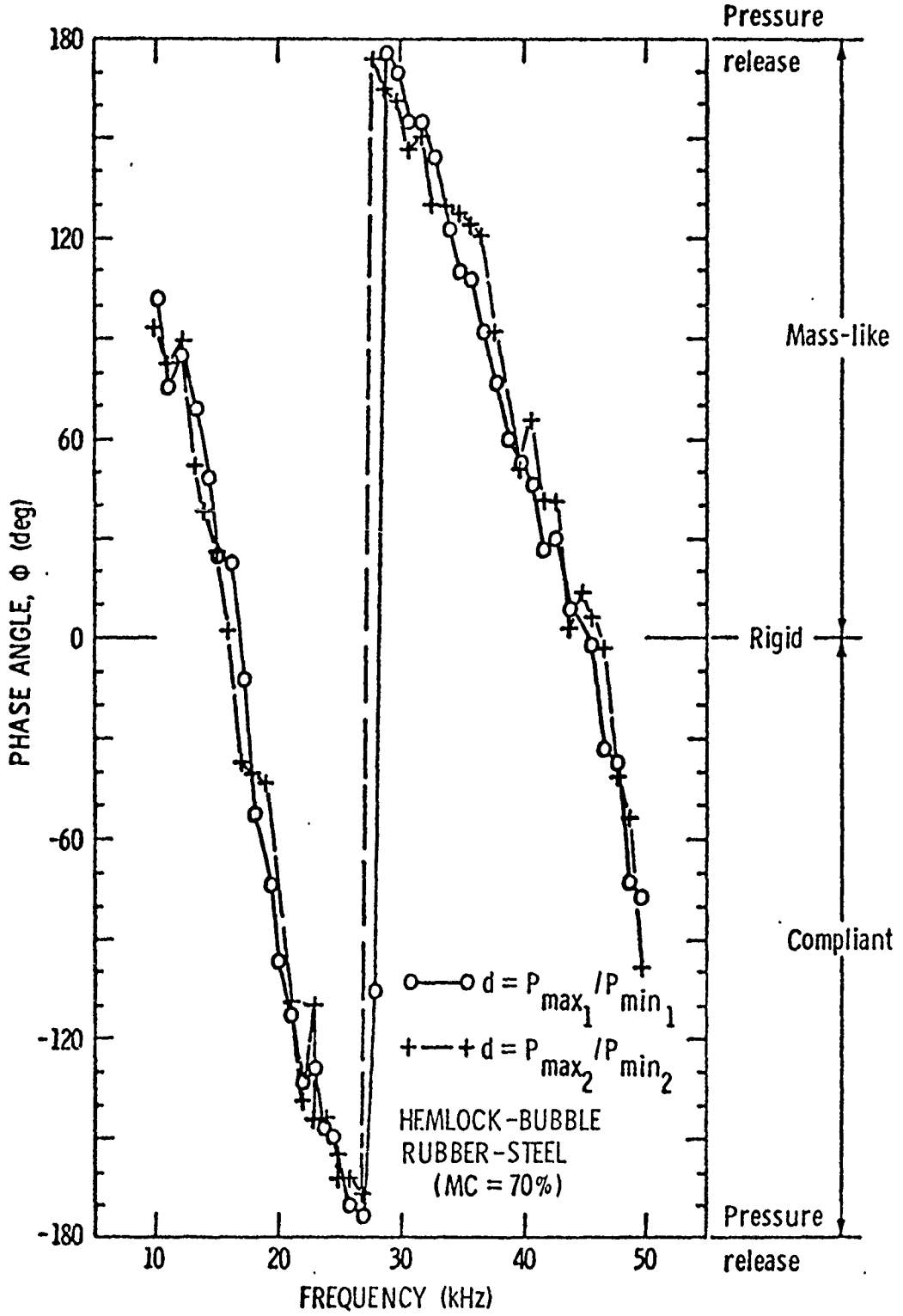

Figure 24. Phase Angle Versus Frequency for Hemlock-Bubble Rubber Steel.

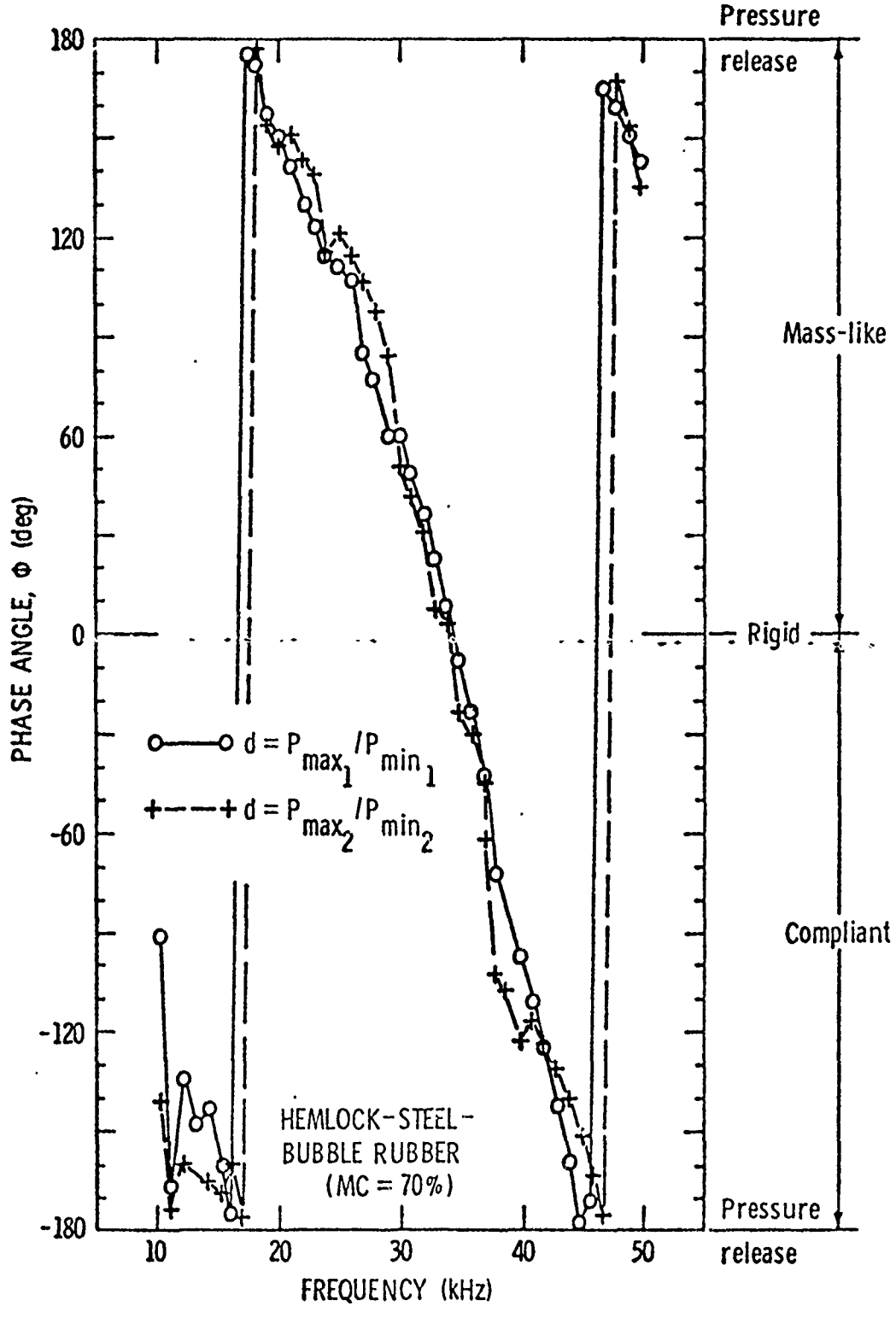

Figure 25. Phase Angle Versus Frequency for Hemlock-Steel-Bubble Rubber.

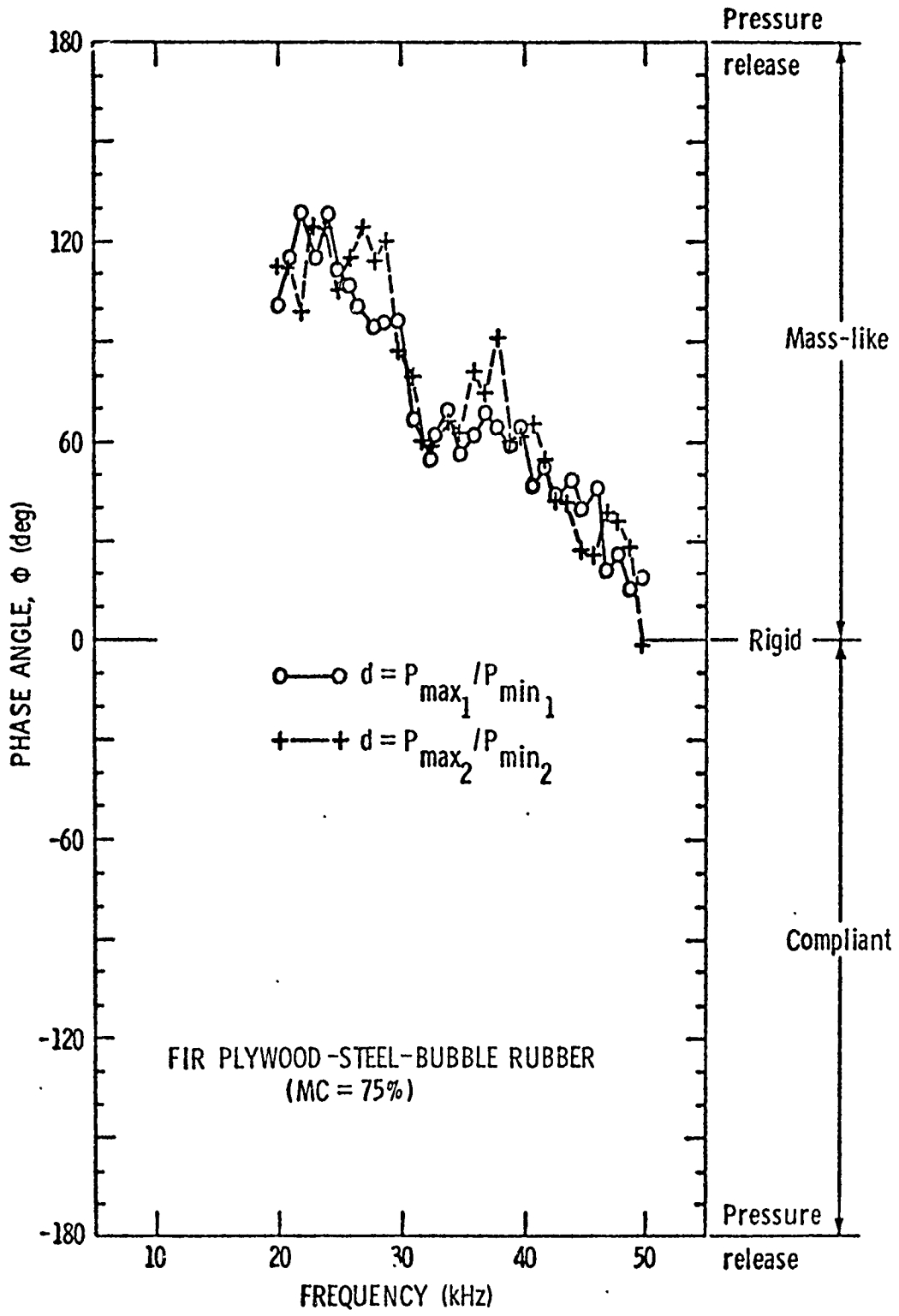

Figure 26. Phase Angle Versus Frequency for Fir Plywood-Steel-Bubble Rubber.

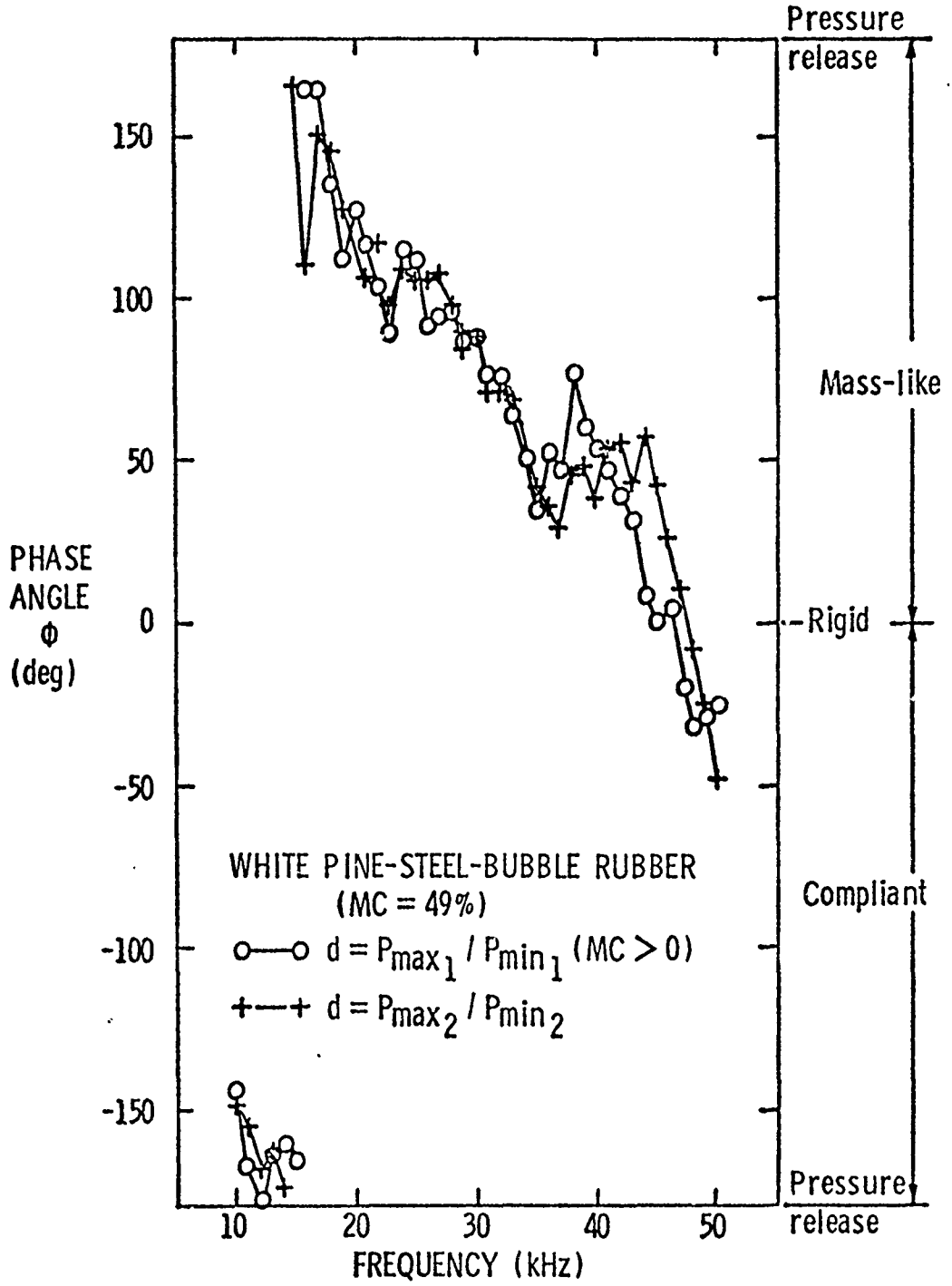

Figure 27. Phase Angle Versus Frequency for White Pine (MC 49 Percent)-Steel-Bubble Rubber.

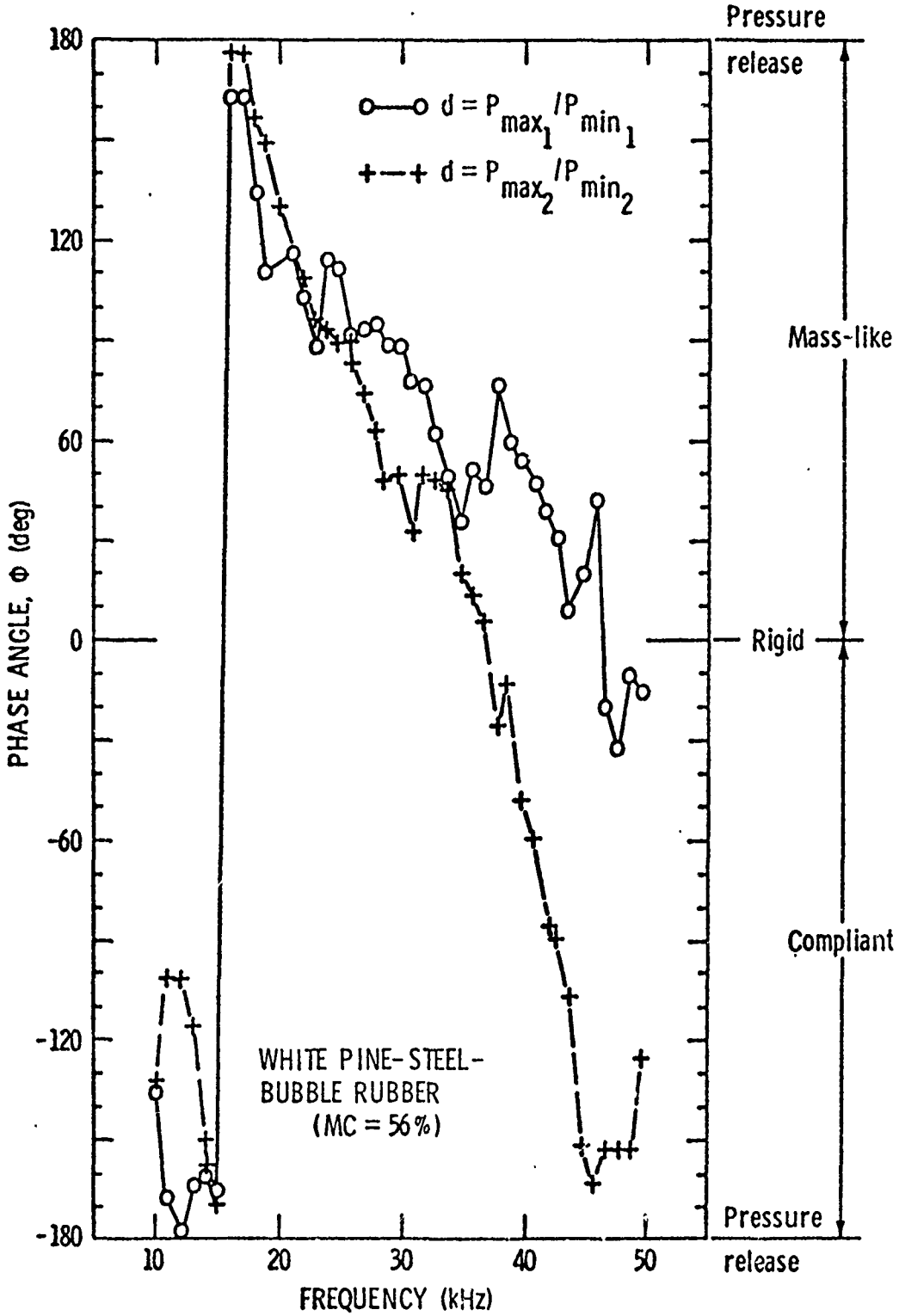

Figure 28. Phase Angle Versus Frequency for White Pine (MC 56 Percent)-Steel-Bubble Rubber.

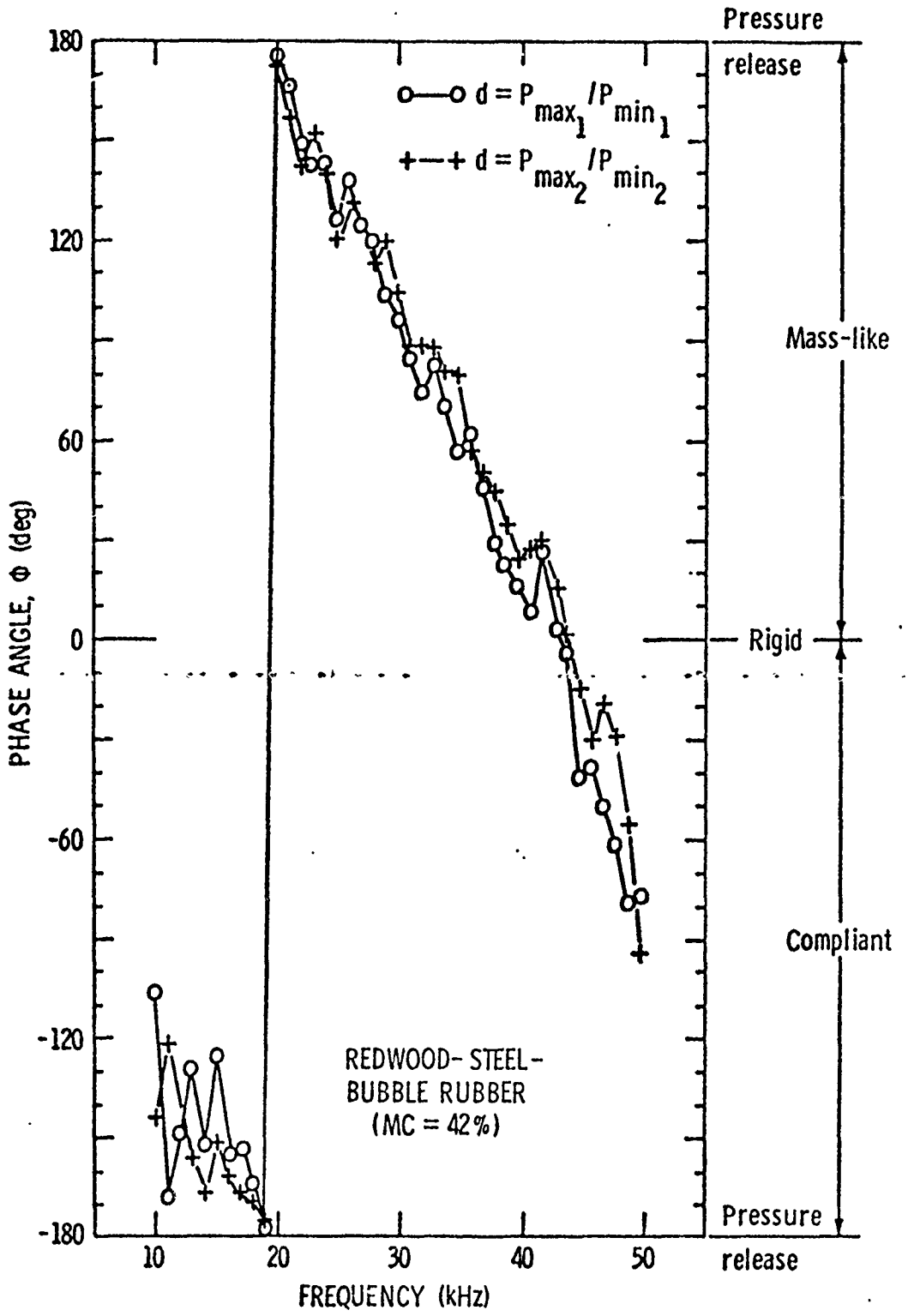

Figure 29. Phase Angle Versus Frequency for Redwood-Steel-Bubble Rubber.

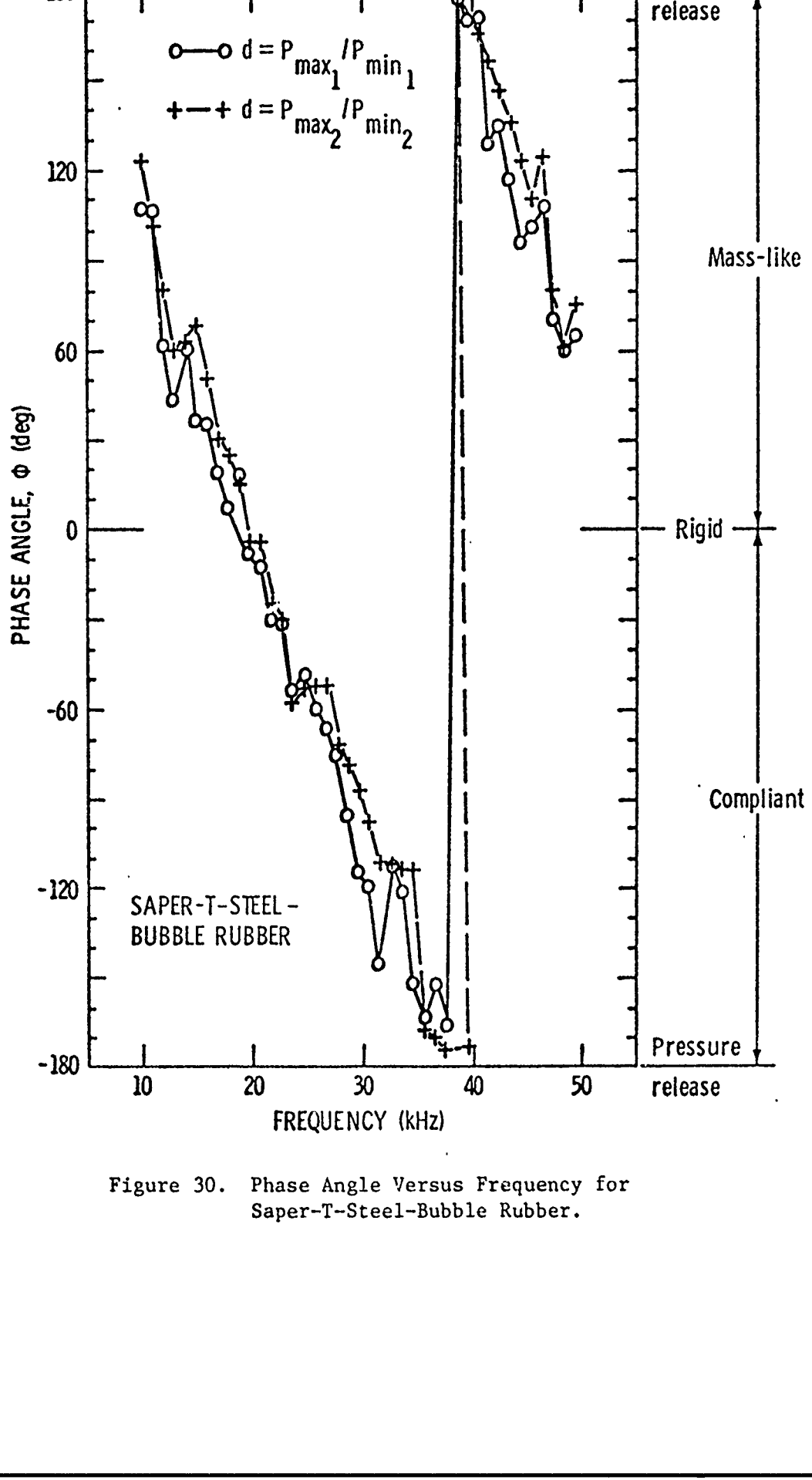

Figure 30. Phase Angle Versus Frequency for Saper-T-Steel-Bubble Rubber.

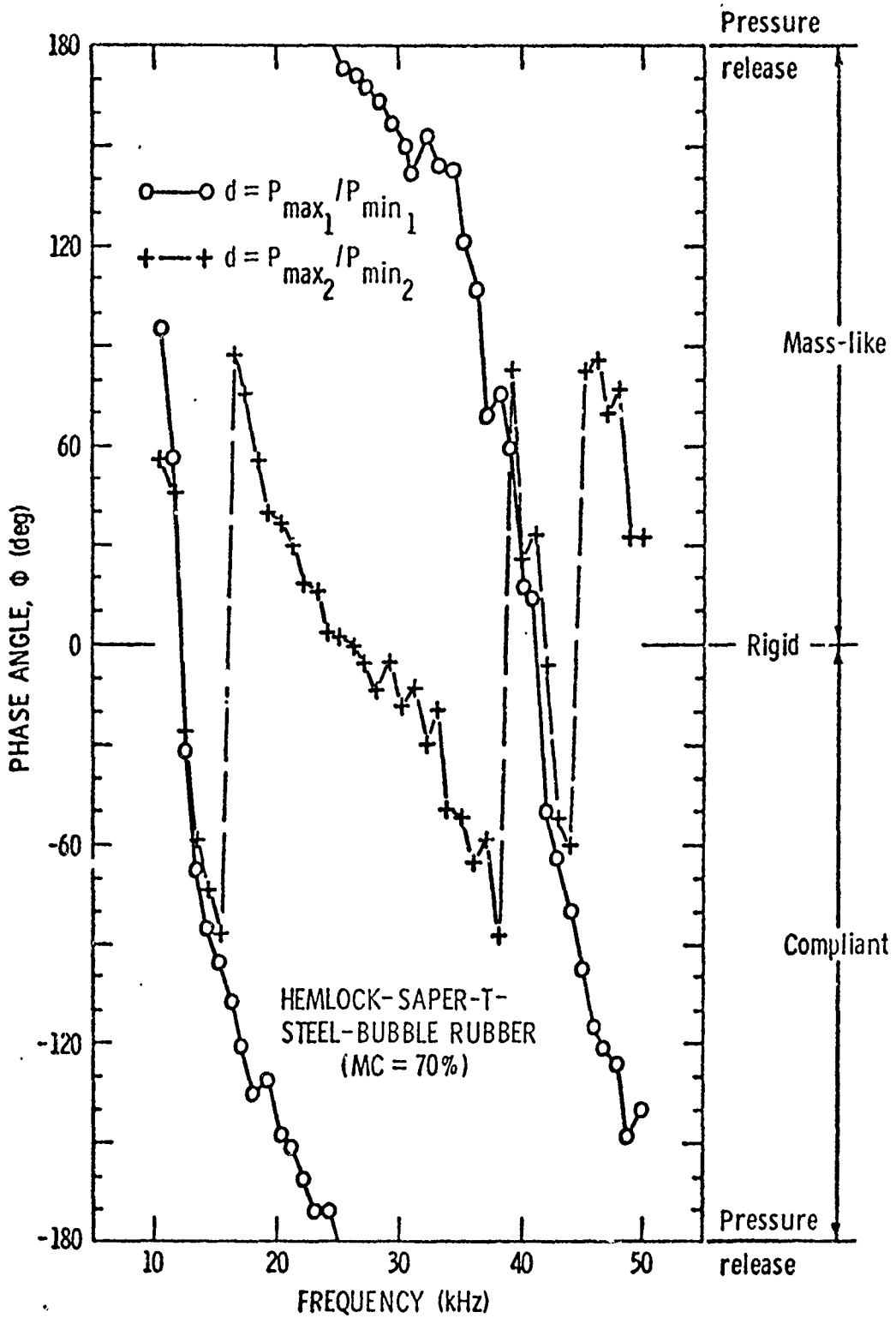

Figure 31. Phase Angle Versus Frequency for Hemlock-Saper-T-Steel-Bubble Rubber

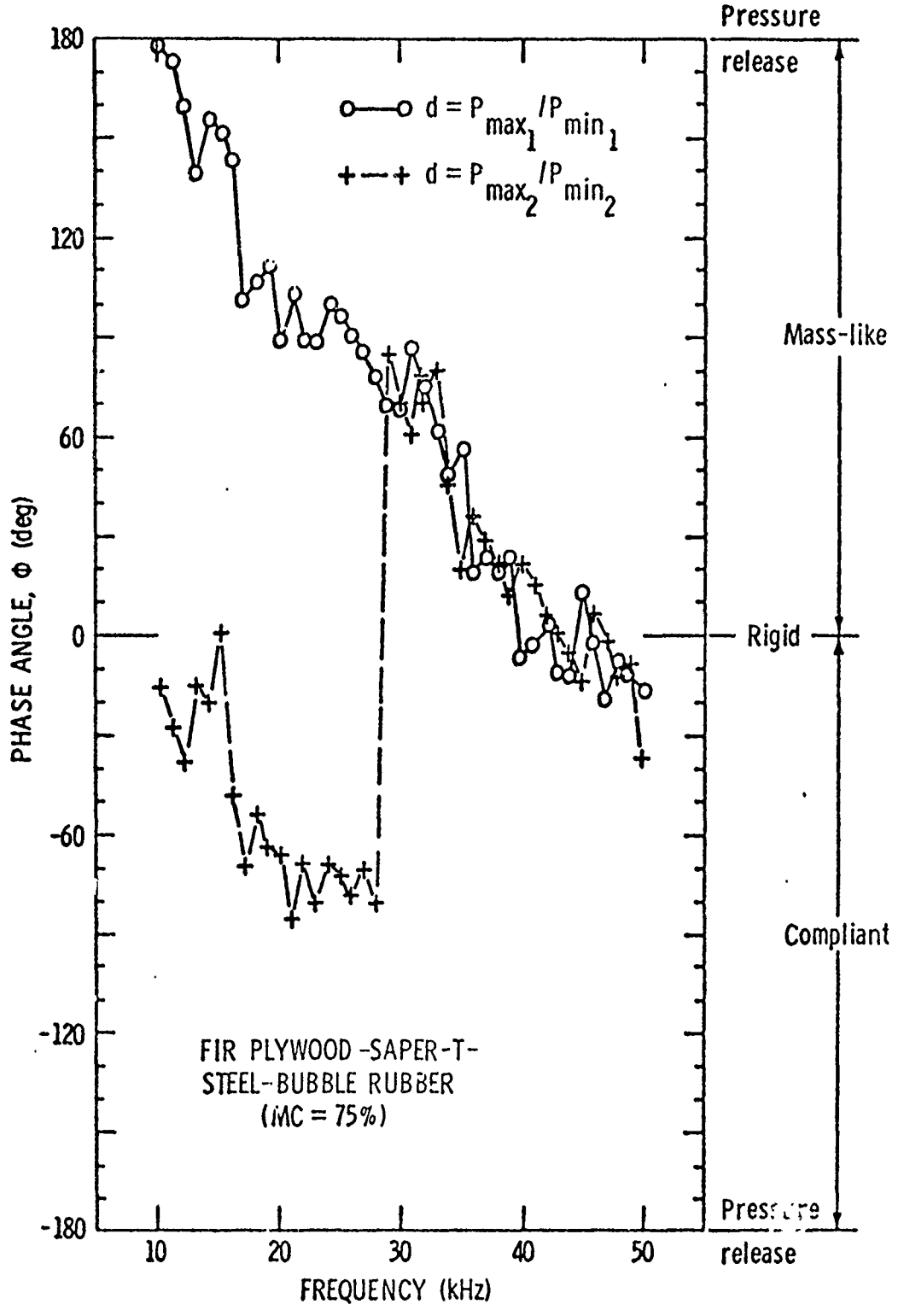

Figure 32. Phase Angle Versus Frequency for Fir Plywood-Saper-T-Steel-Bubble Rubber.

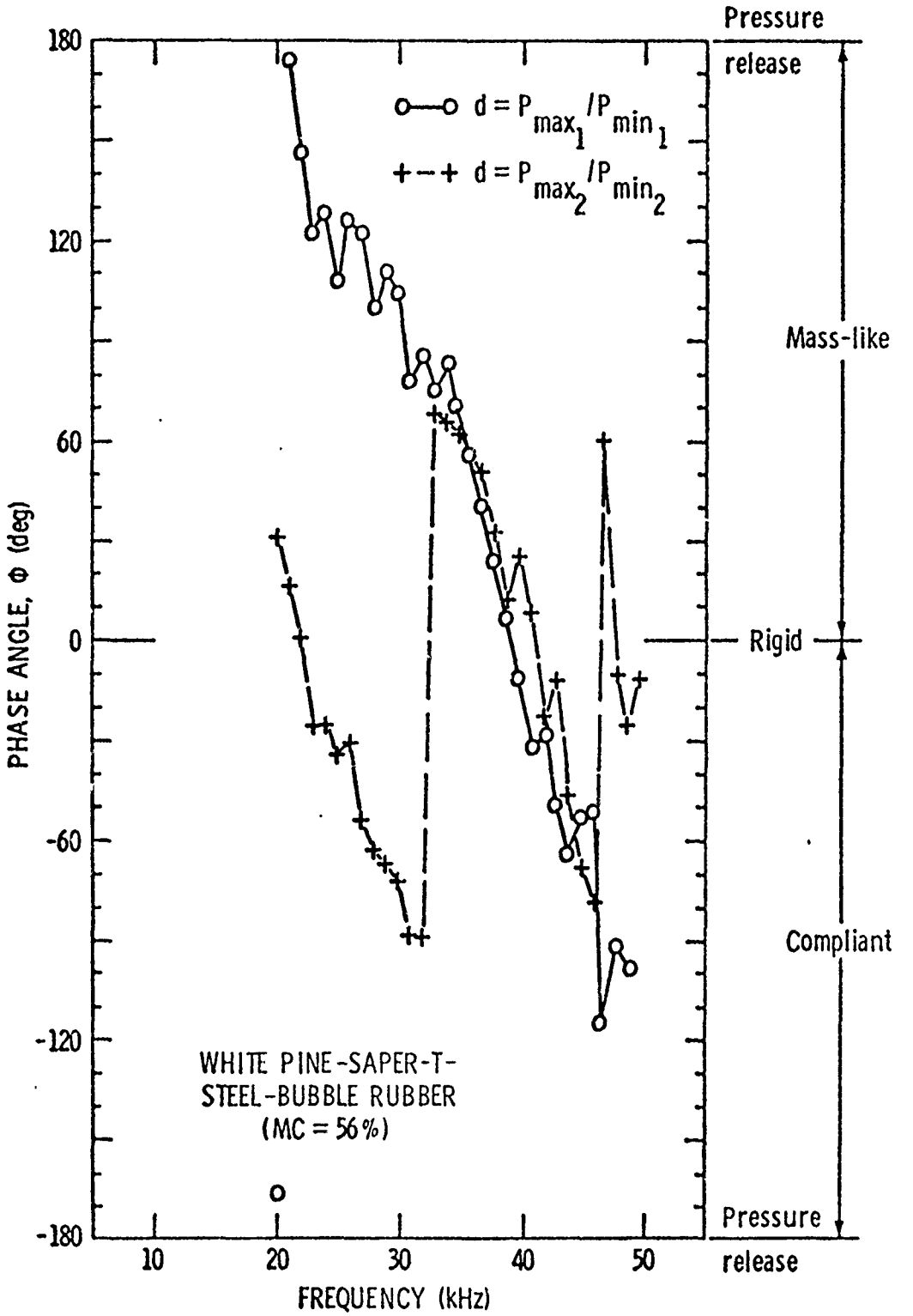

Figure 33. Phase Angle Versus Frequency for White Pine-Saper-T-Steel-Bubble Rubber.

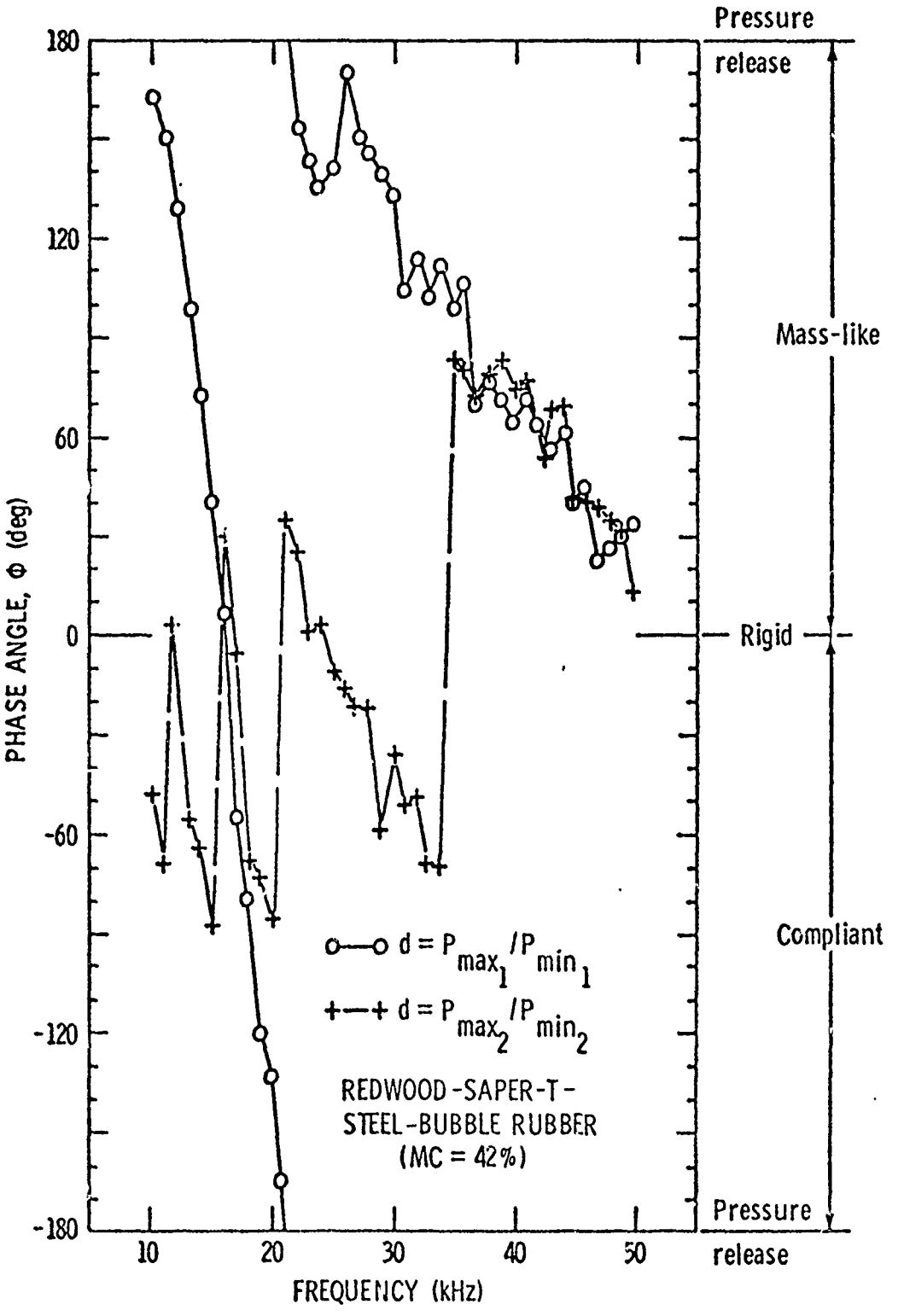

Figure 34. Phase Angle Versus Frequency for Redwood-Saper-T-Steel-Bubble Rubber.

BIBLIOGRAPHY

1. Biot, M. A., "Theory of Propagation of Elastic Waves in a Fluid-Saturated Porous Solid. I. Low-Frequency Range," J. Acoust. Soc. Am., 28, 168-178 (1956).

2. Biot, M. A., "Theory of Propagation of Elastic Waves in a Fluid-Saturated Porous Solid. II. Higher Frequency Range," J. Acoust. Soc. Am., 28, 179-191 (1956).

3. Bobber, R. J., "Underwater Electroacoustic Measurements," U.S. Government Printing Office, LCC Card No. 72-608304 (1970).

4. Cops, A. and Myncke, H., "Determination of Sound Absorption Coefficients Using a Tone-Burst Technique," Acustica, 29 (1973).

5. Cramer, W. S. and Johnson, T. F., "Underwater Sound Absorbing Structures," J. Acoust. Soc. Am., 28, 501-502(L) (1956).

6. Cramer, W. S., "Sound-Absorbing Linings for Water-Filled Tanks," Sound, 2 (1963).

7. Darner, C. L., "An Anechoic Tank or Underwater Sound Measurements at High Hydrostatic Pressure," J. Acoust. Soc. Am., 26, 211 (1954).

8. English, B. V. and Darner, C. L., "Reduction of Reverberation in a Water-Filled Steel Test Vessel by Use of a Porous Material," J. Acoust. Soc. Am., 20, 587(A) (1948).

9. Handbook of Products, "Materials for Underwater Sound Application," Second Edition, B. F. Goodrich Aerospace and Defense Products, Akron, Ohio (1961).

10. Ivanov, V. V., Medvedev, Yu. A., and Stepanov, B. M., "Sound Propagation in a Wet Porous Medium," Soviet Physics - Acoustics, 14, 51-53 (1968).

11. Kinsler, L. E. and Frey, A. R., Fundamentals of Acoustics, John Wiley and Sons, Inc., New York (1962).

12. Lastinger, J. L., "Acoustic Characteristics of Woods at High Hydrostatic Pressure," J. Acoust. Soc. Am., 47, 285-289 (1970).

13. Marboe, R. F. and Farwell, R. W., "Absorption and Reflection Characteristics of a Water-Filled Anechoic Tank," J. Acoust. Soc. Am., 31. 1573(A) (1959).

14. Mason, W. P. and Hibbard, F. H., "Absorbing Media for Underwater Sound Measuring Tanks and Baffles," J. Acoust. Soc. Am., 20, 476-482 (1948).

15. Meyer, E. (Ed.) Sound Absorption and Sound Absorbers in Water, Department of the Navy, Bureau of Ships, NASHIPS 900, Vol. 1, 164 (1950).

16. Mikeska, E. E. and Behrens, J. A., "Evaluation of Transducer Window Materials," J. Acoust. Soc. Am., 59, 6 (1976).

17. Okushima, M., "A New Tube Method for Measuring Complex Pressure Reflection Coefficients of Absorbers in Water," J. Acoust. Soc. Jap., 17, 213-222 (1961). In Japanese.

18. Panshin, A. J. and Zeeuw, de Carl, Textbook of Wood Technology, McGraw-Hill Book Co., New York (1966).

19. Purcell, W. E., "Materials for Noise and Vibration Control," Sound and Vibration, 10 (1976).

20. Richardson, E. G., Technical Aspects of Sound, Elsevier Publishing Co., New York, Vols. I & II (Chapter 5 & 6) (1957).

21. Rubega, R. A. and Culver, A., "Some Experiments in Underwater Sound Absorption," J. Acoust. Soc. Am., 33, 1680(A) (1961).

22. Skudrzyk, E. J., The Foundation of Acoustics: Basic Mathematics and Basic Acoustics, Springer-Verlag, New York, Wien (1971).

23. Tamarkin, P. and Eby, R. K., "Tank Wall Lining for Underwater Sound Use," J. Acoust. Soc. Am., 27, 692-698 (1955).

APPENDIX

The "Moisture Content" may be defined by:

$$MC = \frac{W_{wet} - W_{dry}}{W_{dry}} \quad ,$$

where W_{dry} = air-dried weight, and W_{wet} = absorbed weight. Note that W_{dry} is not the oven-dried weight but is the weight for the wood under atmospheric conditions.

DISTRIBUTION LIST FOR UNCLASSIFIED TM 78-52 by Felicia Antonina Barge
dated May 1978

Commander
Naval Sea Systems Command
Department of the Navy
Washington, DC 20362
Attn: Library
Code NSEA-09G32
(Copies No. 1 and 2)

Naval Sea Systems Command
Attn: A. V. Bress
Code NSEA-03
(Copy No. 3)

Naval Sea Systems Command
Attn: C. G. McGuigan
Code NSEA-03133
(Copy No. 4)

Naval Sea Systems Command
Attn: L. Benen
Code NSEA-0322
(Copy No. 5)

Naval Sea Systems Command
Attn: E. J. McKinney
Code NSEA-0342
(Copy No. 6)

Naval Sea Systems Command
Attn: E. G. Liszka
Code NSEA-0342
(Copy No. 7)

Naval Sea Systems Command
Attn: G. Sorkin
Code NSEA-035
(Copy No. 8)

Naval Sea Systems Command
Attn: T. E. Peirce
Code NSEA-0351
(Copy No. 9)

Naval Sea Systems Command
Attn: J. G. Juergens
Code NSEA-037
(Copy No. 10)

Naval Sea Systems Command
Attn: H. C. Claybourne
Code NSEA-0371
(Copy No. 11)

Naval Sea Systems Command
Attn: A. R. Paladino
Code NSEA-0372
(Copy No. 12)

Naval Sea Systems Command
Attn: D. Creed
Code NSEA-03132A
(Copy No. 13)

Naval Sea Systems Command
Attn: C. Taylor
Code NSEA-037
(Copy No. 14)

Commander
Naval Ship Engineering Center
Department of the Navy
Washington, DC 20360
Attn: W. L. Louis
Code NSEC-6136B
(Copy No. 15)

Naval Ship Engineering Center
Attn: R. J. Cauley
Code NSEC-6140B
(Copy No. 16)

Naval Ship Engineering Center
Attn: F. Welling
Code NSEC-6144
(Copy No. 17)

Naval Ship Engineering Center
Attn: R. M. Petros
Code NSEC-6148
(Copy No. 18)

Naval Ship Engineering Center
Attn: D. Burke
Code NSEC-6113C1
(Copy No. 19)

Commanding Officer
Naval Underwater Systems Center
Newport, RI 02840
Attn: Technical Director
Code SB3
(Copy No. 20)

Naval Underwater Systems Center
Attn: D. Goodrich
Code SB323
(Copy No. 21)

Naval Underwater Systems Center
Attn: R. Nadolink
Code SB323
(Copy No. 22)

Naval Underwater Systems Center
Attn: R. Trainor
Code SB323
(Copy No. 23)

Naval Underwater Systems Center
Attn: F. White
Code SB332
(Copy No. 24)

Naval Underwater Systems Center
Attn: Library
Code LA15
(Copy No. 25)

Commanding Officer
Naval Ocean Systems Center
San Diego, CA 92152
Attn: Library
(Copy No. 26)

Naval Ocean Systems Center
Attn: J. W. Hoyt
Code 2501
(Copy No. 27)

Naval Ocean Systems Center
Attn: D. Nelson
Code 2542
(Copy No. 28)

Naval Ocean Systems Center
Attn: A. G. Fabula
Code 5311
(Copy No. 29)

Commanding Officer and Director
David W. Taylor Naval Ship R&D Center
Department of the Navy
Bethesda, MD 20084
Attn: Library
(Copy No. 30)

David W. Taylor Naval R&D Center
Attn: W. E. Cummins
Code 15
(Copy No. 31)

David W. Taylor Naval R&D Center
Attn: S. F. Crump
Code 1505
(Copy No. 32)

David W. Taylor Naval R&D Center
Attn: W. B. Morgan
Code 154
(Copy No. 33)

David W. Taylor Naval R&D Center
Attn: R. Cumming
Code 1544
(Copy No. 34)

David W. Taylor Naval R&D Center
Attn: J. McCarthy
Code 1552
(Copy No. 35)

David W. Taylor Naval R&D Center
Attn: Y. T. Shen
Code 1524
(Copy No. 36)

David W. Taylor Naval R&D Center
Attn: M. Sevik
Code 19
(Copy No. 37)

David W. Taylor Naval R&D Center
Attn: W. K. Blake
Code 1942
(Copy No. 38)

David W. Taylor Naval R&D Center
Attn: R. W. Brown
Code 1942
(Copy No. 39)

Commanding Officer and Director
David W. Taylor Naval Ship R&D Center
Department of the Navy
Annapolis Laboratory
Annapolis, MD 21402
Attn: J. G. Stricker
Code 2721
(Copy No. 40)

DISTRIBUTION LIST FOR UNCLASSIFIED TM 78-52 by Felicia Antonina Barge
dated May 1978 (continued)

Commander Naval Surface Weapon Center
Silver Spring, MD 20910
Attn: Library
(Copy No. 41)

Naval Surface Weapon Center
Attn: G. C. Gaunaurd
(Copy No. 42)

Office of Naval Research
Department of the Navy
800 N. Quincy Street
Arlington, VA 22217
Attn: H. Fitzpatrick
(Copy No. 43)

Defense Documentation Center
5010 Duke Street
Cameron Station
Alexandria, VA 22314
(Copies No. 44 to and
including 55)

National Bureau of Standards
Aerodynamics Section
Washington, DC 20234
Attn: P. S. Klebanoff
(Copy No. 56)

National Bureau of Standards
Attn: D. S. Pallet
(Copy No. 57)

Rand Corporation
1700 Main Street
Santa Monica, CA 90406
Attn: R. King
(Copy No. 58)

Rand Corporation
Attn: C. Gazley
(Copy No. 59)

Applied Research Laboratory
The Pennsylvania State University
Post Office Box 30
State College, PA 16801
Attn: W. Thompson, Jr.
(Copy No. 60)

Applied Research Laboratory
Attn: E. J. Skudrzyk
(Copy No. 61)

Applied Research Laboratory
Attn: H. M. Frost
(Copy No. 62)

Applied Research Laboratory
Attn: G. C. Lauchle
(Copy No. 63)

Applied Research Laboratory
Garfield Thomas Water Tunnel Library
(Copy No. 64)